中图分类号：TP274

论 文 编 号 ：10006SLS1925204

北京航空航天大學

# 硕 士 学 位 论 文

# 高精度 GNSS 数据处理方法及地震位移测量应用研究

作 者 姓 名　　蒙多扎

学 科 专 业　　信息与通信工程(空间技术应用)

指 导 教 师　　施闯

培 养 院 系　　国际学院

# High Accuracy GNSS Data Processing and Determination of Displacement by Earthquake

A Dissertation Submitted for the Degree of Master

**Candidate: Mario Cesar Mendoza Del Aguila**

**Supervisor: Prof. Dr. Shi Chuang**

International School

Beihang University, Beijing, China

**中图分类号：TP274**

**论 文 编 号 ：10006LS1925204**

硕 士 学 位 论 文

# 高精度 GNSS 数据处理及地震位移监测应用研究

作者姓名　　蒙多扎　　申请学位级别　　工学硕士

指导教师姓名　　施闯　　职　　称　　教　授

学科专业　　信息与通信工程(空间技术应用)　　研究方向　　卫星导航

学习时间自　2019　　年　9 月　15 日　　起至　2021　　年　　月　　日止

论文提交日期　2021 年　5　月　　日　论文答辩日期　2021 年　　月　　日

学位授予单位　　北京航空航天大学　　学位授予日期　　年　　月　　日

# 关于学位论文的独创性声明

本人郑重声明：所呈交的论文是本人在指导教师指导下独立进行研究工作所取得的成果，论文中有关资料和数据是实事求是的。尽我所知，除文中已经加以标注和致谢外，本论文不包含其他人已经发表或撰写的研究成果，也不包含本人或他人为获得北京航空航天大学或其它教育机构的学位或学历证书而使用过的材料。与我一同工作的同志对研究所做的任何贡献均已在论文中作出了明确的说明。

若有不实之处，本人愿意承担相关法律责任。

学位论文作者签名：  　　日期：　2021 年 10 月 29 日

# 学位论文使用授权书

本人完全同意北京航空航天大学有权使用本学位论文（包括但不限于其印刷版和电子版），使用方式包括但不限于：保留学位论文，按规定向国家有关部门（机构）送交学位论文，以学术交流为目的赠送和交换学位论文，允许学位论文被查阅、借阅和复印，将学位论文的全部或部分内容编入有关数据库进行检索，采用影印、缩印或其他复制手段保存学位论文。

保密学位论文在解密后的使用授权同上。

学位论文作者签名：  　　日期：　2021 年 10 月 29 日

指导教师签名：_____　　日期：　2021 年 10 月 29 日

# 摘　　要

秘鲁位于南美洲的西部边缘，处于纳斯卡板块与南美洲板块的交汇处，地壳运动的能量在这里产生了积累，最终导致了南美洲的地震运动与位移。

对于板块运动和变形而引起的位移，可以使用 GNSS 技术进行直接测量，这是了解这些运动学原理的基本手段。使用卫星大地测量技术，通过分析来自秘鲁国家地理研究所 (IGN) 的秘鲁大地连续监测网络 (REGPMOC) 连续跟踪站的 GNSS 数据，可以得到主要由纳斯卡板块和南美洲板块相互作用而产生的秘鲁边缘位移率。

世界协调时 2019 年 5 月 26 日 7 时 41 分 14 秒（当地时间 2 时 41 分 14 秒），位于利马东北部约 720 公里处的秘鲁东部地区发生里氏 8.0 级地震。这次地震是由于纳斯卡板块的中深度正断层破裂造成的。震源位于南纬 5.796°，西经 75.298°，震源深度 109.9 公里 (USGS, 2019)。美国地质调查局 (USGS) 提供的震源机制解表明，破裂发生于一个南北向的中度倾斜正断层上。秘鲁位于纳斯卡板块的俯冲带内，板块在该地区以每年约 7 厘米（约 2.7 英寸/年）的速度相对于南美板块向东俯冲。中等深度的俯冲事件在秘鲁北部和南美洲西部较为常见。与类似震级的浅源地震相比，它们通常对震源上方地表造成的破坏较小，但在距离震中较远的地区仍可有较大震感 (USGS, 2019)。本次地震在秘鲁、厄瓜多尔、哥伦比亚、委内瑞拉和巴西多地产生震感。

本文的研究区域包括秘鲁的丛林区域（主要是发生 8 级地震的区域）。为比较每个 GNSS 站在地震前后的位置，本文使用了 14 个环绕震中的 GNSS 站，分析分离距离（基线）并得出位移矢量（震级和方向）。本文采用地震前一周和后一周的 GNSS 数据（已知地震日为 146 儒略日），即 139 儒略日到 156 儒略日。使用 GNSS 处理软件 PANDA（由中国武汉大学开发的用于 GNSS 数据分析的精密软件包）来获取实验结果。结果显示，在毫米级精度上，地震附近的 GNSS 测站向西北方向发生了大约 2 厘米的位移。

**关键词**：GNSS，PANDA，ITRF，精密单点定位，最小二乘法

# Abstract

Peru is located along the western margin of South America, between the convergence of the Nazca and South American tectonic plates, where efforts and energy accumulation are generated. The consequence of which are seismic movements and displacements on the South American continent.

The use of GNSS technology provides direct measurements of the displacements due to the movement of the plates and the deformation, basic information for the understanding of the kinematics of the movements. Using satellite geodesy techniques, Peruvian margin displacement rates produced mainly by the interaction between the Nazca and South American plates have been derived by analysis of GNSS data from the GNSS Permanent Tracking Stations of the Peruvian Geodetic Continuous Monitoring Network (REGPMOC) of the Geographic Institute National (IGN) of Peru.

On Sunday May 26, 2019, at 7:41:14 UTC (2:41:14 local time), a magnitude (Mw) 8.0 earthquake took place in Eastern Perú approximately 720 km northeast of Lima. The earthquake occurred as the result of an intermediate-depth normal faulting rupture of the Nazca plate. The hypocenter of the earthquake was located at 5.796°S 75.298°W at a depth of 109.9 km (USGS, 2019). Focal mechanism solutions provided by the U.S. Geological Survey (USGS) indicate that the rupture occurred on either a north- or south-striking, moderately dipping normal fault. Perú is located within the subduction zone of the Nazca plate which subducts in an eastern downward motion relative to the South America plate in this region at a velocity of approximately 7 cm/yr (about 2.7 inch/yr). Intermediate-depth subduction events are relatively common in northern Perú and western South America. They typically cause less damage on the ground surface above their foci than similar magnitude shallow-focus earthquakes, but large intermediate-depth earthquakes may be felt at great distance from their epicenters (USGS, 2019). The earthquake was felt by people in Perú, Ecuador, Colombia, Venezuela and Brazil.

The study area includes the Peruvian jungle area, mainly the area where the 8-magnitude earthquake occurred. The same GNSS stations have been used for the purpose of making comparisons of the position of each GNSS station before and after the earthquake, in this research used 14 GNSS stations rounding earthquake epicenter, analyzing separation distances (baselines) and obtaining the displacement vectors (magnitude and direction). In this thesis used data GNSS one week before and one week after earthquake, since 139 Julian day to 156 Julian day, knowing earthquake day was in 146 Julian day, data was made quality check and it result good data, according the standard solutions and the made post processing and analysis. Results obtained using the scientific GNSS processing software PANDA, a precision package for GNSS data analysis, developed by the University of Wuhan, China, are shown. The results are high accuracy on millimeters order results obtained are surrounding 2cm displacement on near GNSS stations earthquake, to the north west.

Key words: GNSS, PANDA, ITRF, Precise Point Positioning, Least Squares method

# Contents

# List of Figures

# List of Tables

# 1 Introduction

## 1.1 Background

Nowadays GNSS systems allow us to observe the behavior of our planet, in different areas of the application of geospatial sciences. GNSS information can be used for a better understanding of the behavior of our planet. For the particular case, to study the behavior of surface displacements, it is necessary to use high precision measuring instruments. GNSS receivers allow measuring the position and speed of a point on the earth's surface. For example, an investigation was conducted on the CORS Reference Displacement Monitoring Stations using GNSS precise point positioning in Peru showing use of the GNSS technology allows for achieving high accuracy displacements [1], as well as research was carried out on the analysis of the geodesic network displacement where it is shown the statistical significance of point displacements in the geodetic network as the intermediate stage between the adjustment of respective epochs measurements and an in-depth deformation analysis [2]. For to do this type of research is necessarily know that basics concepts of reference system [3] and reference frame [4], also GNSS can give us information for study crustal deformation and know GPS velocity field, this uses the velocity field to update geodetic estimates of slip rates of the major structures in the region, compare those for the major Tibetan strike-slip faults against available geological estimates, critically assess any apparent discrepancies, and conclude that there is a good correspondence between geological and geodetic slip rates [5]. About the topics referred before there are many information for have a reference and develop my thesis tentative, in order to obtain results in my research thesis is necessary to use highly robust software that is available to process this information, such as PANDA software, GAMIT or BERESE [6]. Throughout the world there are more than 500 permanent GNSS stations, forming a GNSS network, which defines the systems and world reference frames. As in the world there are global GNSS receivers in Peru there are local GNSS receivers. At present there are 70 GNSS receivers in continuous operation, operating 24 hours a day, all year round; These make up a GNSS network that serves to monitor the Peruvian territory. For this work, the processing and analysis of behavior and displacement will be carried out using

high precision processing with data one week before and after of seismic, using the PANDA scientific software, I will use PANDA software in research as a most essential scientific tools and the quality control [7] of your result will be evaluated using the statistics of the final data as well as compared to results from other reference software.

Peru has 70 GNSS receivers installed along its territory, these track precise positioning data 24 hours per day and 365 days a year.

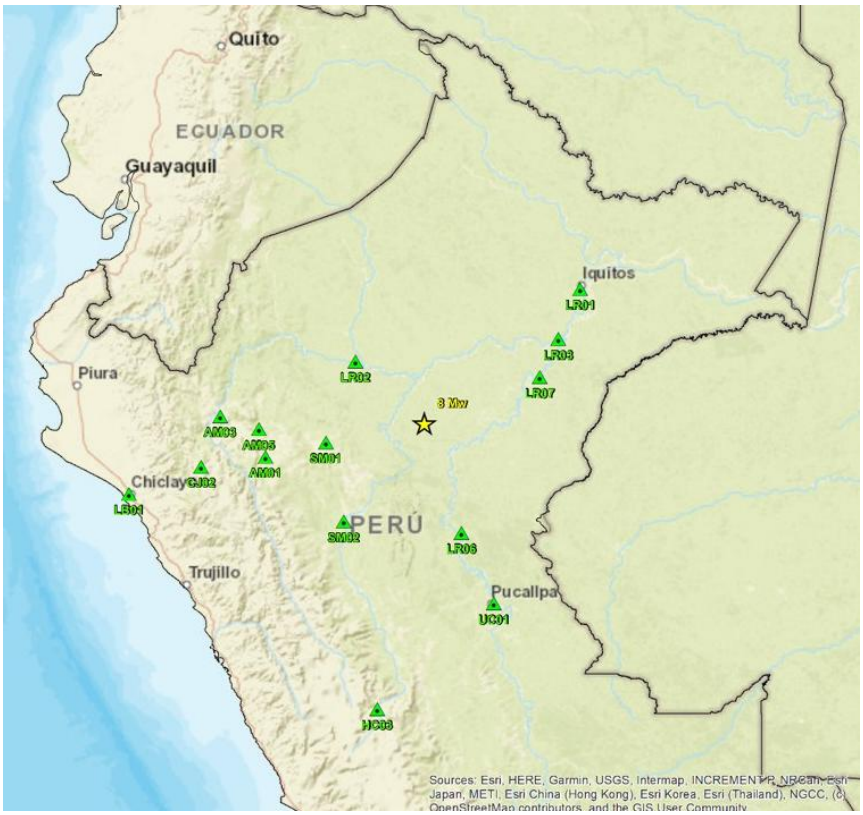


**Figure 1 Location of seismic and GNSS stations**

## 1.2 Research Status

This research was made thanks to National Geographic Institute from Peru, that made possibly get data and information for make easy way this research.

Process GNSS data is important because allow us to knows high accuracy position of GNSS stations, it can show the position and behavior of one point in the earth, and know what is the displacement a long of time.

For this research it used data before and after earthquake for know how many was displacement in 14 GNSS stations points surrounding earthquake, using PANDA software, PANDA used only RINEX data version 2.11 with GPS constellations, and used metadata from

IGS like broadcast, precise ephemeris and clock data.

GPS satellite transmit two frequencies from orbit those are pseudocode and carrier phase observations [8]. GNSS satellite travel on a specific orbit. GNSS technology are significantly of great importance for geodesy and geodynamics. More station will be established and low-Earth-orbiting (LEO) satellites [9] will be connected to GNSS receiver. However, in over the world the number of satellites for example GLONASS system from Russia, Galileo system from Europe and BeiDou from China is going to provide a better precise information to user [10]. International GNSS service (IGS) has provide a better strategy for precise orbit determination (POD) [11]. Precise Point Positioning (PPP) is a high standard geodetic positioning method has provided the sub-decimeter to decimeter level precise positioning accuracy in static and kinematic modes [12]. PPP uses specific GPS satellites in orbit and satellite clock products with un-differenced dual- frequency pseudorange and carrier phase monitoring [13]. Although the sampling interval of 30 s served almost as a standard format to collect GPS data at permanent stations for deformation measurement [14]. GPS seismology uses GPS as displacement seismometers/instruments at a high sampling rate for earthquake study [15]. first successfully detected the high-rate GPS waveforms of displacements caused by the 3 November 2002 Mw7.9 Denali Fault earthquake by using relative GPS positioning techniques to process the 1-Hz GPS data [16].

## 1.3 Dissertation´s Structure

This thesis divided into six main parts, detailed as follows:

- Part one: Introduction

In this part, we presented an overview of the topic of the study, the most important problems, and the importance of monitoring land in earthquake to achieve understand in the study area, motivations, objectives and contents.

- Part two: Literature Review

In this part, we presented the most important concepts in the field of study, the methods used, previous studies and their effectiveness.

- Part three: Methodology and Data Used

In this part, we provided an overview of our study area, the software and data used, and we described the techniques and the methods followed to know the behavior of earthquake, extract raw data convert to rinex and process in PANDA software and analysis the results and changes in earthquake.

- Part four: Applications and Experimental Results

In this part we presented the different steps of the GNSS data preprocessing and the analysis process, as well as the results of the quality check, and application in geodesy and earth sciences.

- Part five: Analysis and Results

In this part we presented the results after processing and quality check, comparison before and after earthquake, displacements, statists. Also, we analyzed and discussed these results, and compared the developments in our study area.

- Part six: Conclusion

In this part we presented the general conclusion of our study which is based on a comprehensive review of the partial and total result.

# 2 Basic Theory

## 2.1 Conventional Terrestrial Reference System and Frame

### 2.1.1 System Definition

Fixed coordinate axes will be used on the Earth, that is, they rotate with it, so that the coordinates of a point, in principle, will always be the same.

The conventions that take the reference system to conventional are:

• Origin: Center of land masses or geocenter, including the atmosphere and oceans.

• Meridian plane: passes through any point on earth and contains the axis of rotation.

• Equator plane: it is perpendicular to the axis of rotation and stops at the geocenter.

• X axis: it is located in the direction of the meridian plane that passes through Greenwich and contained in the equator plane. It is considered internationally as the origin meridian or zero meridian since 1884.

• Y axis: contained in the equator plane and perpendicular to the X axis and its direction will be such that the three axes form a right-handed triplet.

### 2.1.2 Coordinate system

#### 2.1.2.1 Cartesian and spherical coordinates

Any point on the earth's surface will present coordinates (X, Y, Z) in the defined coordinate axis triplet, these points being the ones that constitute the reference frame, figure 2

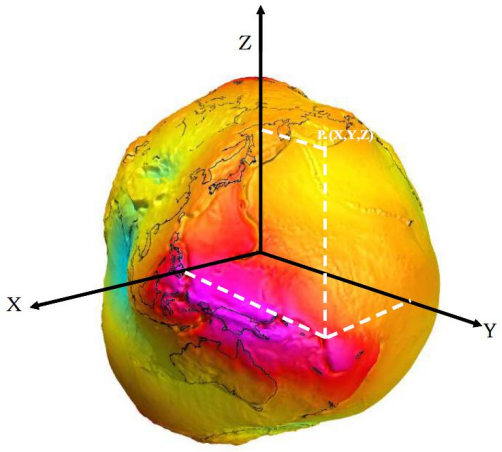


**Figure 2 Cartesian coordinate system [4]**

In any case, it is common to use spherical coordinates for the parameterization of the points on the Earth, (r, φ, λ), figure 3, where, in a generic way, r is the radial distance to the geocenter, φ the geocentric latitude (angle between r and the plane of the equator) and λ the geocentric longitude (angle between the Meridian plane of Greenwich and that of the calculation point, measured in the plane of the equator).

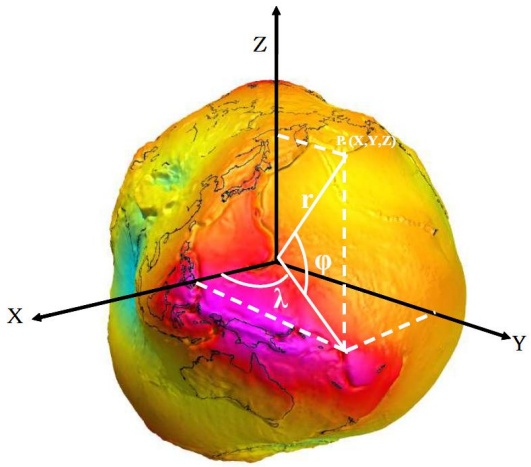


**Figure 3 Spherical coordinate system [4]**

The relationship between spherical and Cartesian coordinates is a matrix product corresponding to the regular parametrization of the sphere:

$$\begin{pmatrix} X \\ Y \\ Z \end{pmatrix} = r \begin{pmatrix} \cos\lambda\cos\varphi \\ \sin\lambda\cos\varphi \\ \sin\varphi \end{pmatrix} \tag{2.0}$$

For the correct definition of the radial distance r (different distance for each point on the Earth and that does not follow any exact geometric pattern), a reference surface must be entered as an approximation to the real shape of the Earth.

### 2.1.2.2 Geographic coordinate system

In first approximation the Earth is a homogeneous sphere of radius R.

The axis of rotation cuts the earth's surface at two points: the North geographic pole (PN) and at the South geographic pole (PS). The North geographic pole is the one from which if the Earth is observed towards its interior, it is rotated in the opposite direction to the needles of the clock, figure 4.

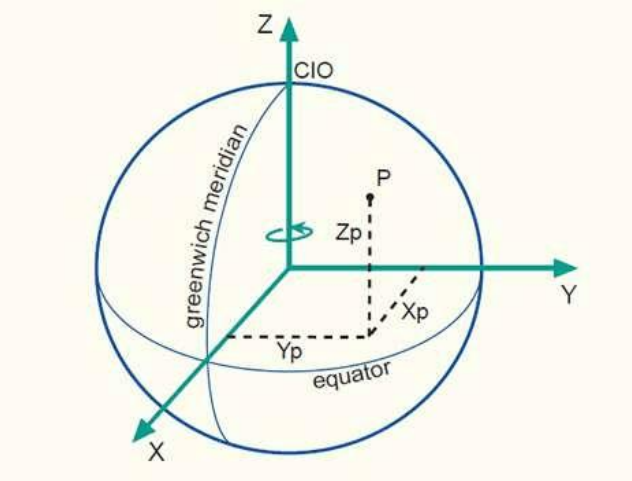


**Figure 4 Spherical approach to the Earth [4]**

The vertical of any point on the Earth's surface will pass through the center of the Earth.

The position of a point E on the Earth's surface is determined by two coordinates, figure 5.

The geographical latitude (φ) from point E is called the angle that the vertical of E makes with the plane of the Earth's equator. Geographic latitude varies from 0º to 90º in the boreal hemisphere (northern latitude) and from 0º to -90º in the southern hemisphere (southern latitude).

The geographic longitude (λ) of point E is called the angle that the meridian of the point forms with the origin meridian. Geographic longitude varies from 0º to 180º in the eastern hemisphere and from 0º to -180º in the western hemisphere, that is, the first to the east and the second to the west.

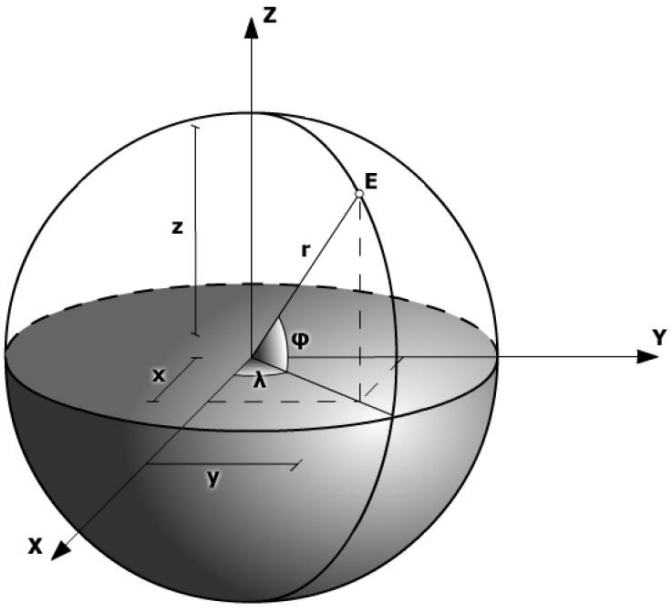


**Figure 5 Geographical coordinates [4]**

### 2.1.2.3 Geodetic and geocentric coordinate system. Geodetic reference system

The second approximation to the shape of the Earth is an ellipsoid of revolution defined by its semi-major axis (a) and its semi-minor axis (b) or flattening (f). The center of the ellipsoid coincides with the center of the reference system, that is, with the geocenter and the semi-minor axis is made to coincide with the Earth's axis of rotation, thus constituting the geodetic coordinate system.

The geodesic vertical at a point on the surface of the ellipsoid of revolution coincides with the direction of the vector normal to the ellipsoid at that point, and therefore does not pass through the center of the ellipsoid, figure 6.

So, the geodetic coordinates will be:

Geodetic latitude: it is the angle formed by the geodetic vertical of the point with the geodesic equator plane.

Geodetic longitude: it is the angle formed by the geodetic meridian of the calculation point and the origin geodetic meridian.

We introduce at this moment the geocentric coordinates since, on the ellipsoid they will not coincide with the geodesics, in this case the geocentric longitude will be equal to the geodesic, but the geocentric latitude (β) will be the angle between the line that joins the center of the ellipsoid and a point on the ellipsoid and the geodesic equator.

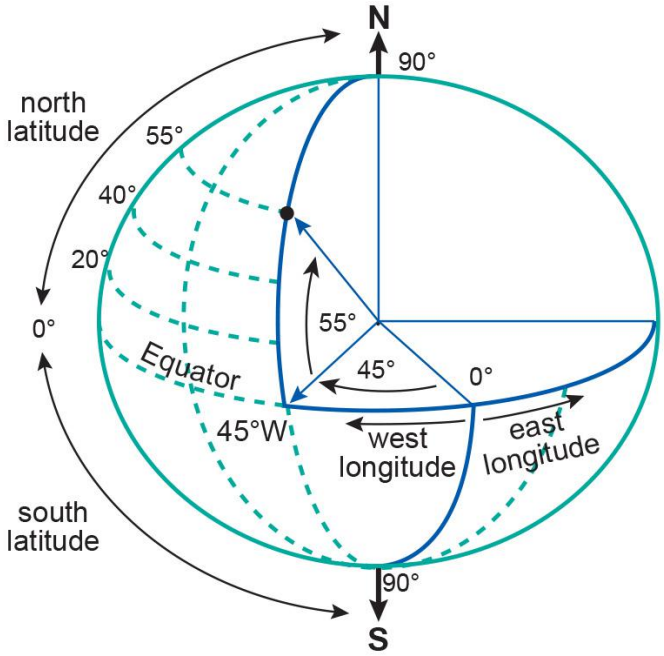


**Figure 6 Geodetic and geocentric coordinates [4]**

### 2.1.3 Geodesic reference system

#### 2.1.3.1 Global geodetic reference systems. GRS and WGS84

Datum will be defined as the set of parameters that define the position of an ellipsoid with respect to the earth. To determine it, it is necessary to know the geometry of the ellipsoid a and f, its position with respect to the geocenter ΔX, ΔY, ΔZ (coordinates of the center of the ellipsoid with respect to the geocenter), its orientation R1, R2, R3 (orientation of the ellipsoid axes with respect to the terrestrial ones) and the k scale.

If $\Delta X = \Delta Y = \Delta Z = 0$, the Geodetic datum is called Global or absolute.

The Geodetic Reference System 1980 (GRS80) adopted by the IUGG (International Union of Geodesy and Geophysics) by its general assembly in Canberra in 1979, belongs to this group.

This system replaces the GRS67 for not adequately representing the size, shape and gravitational field with sufficient precision for most geodetic, geophysical, astronomical and hydrographic applications.

The main parameters of the system are:

a = 6378137 m. (Obtained from SLR and Doppler measurements).

J2 = 108263 · 10-8 (Obtained from disturbances in the orbit of satellites).

GM = 3986005108 m3 / sg2 (Obtained from SLR, LLR and spatial tests).

ω = 7293115 · 10-11 rd / sg (Obtained from astronomical measurements).

The orientation of the Z axis will be that defined by the C.I.O. pole, as the X axis the meridian 0 defined by the B.I.H. and the Y axis forming the right-handed triplet.

This system is still in force and its definition has not been updated since it must be taken into account that below the meter in the difference of parameters, there is no practical difference in the determination of coordinates. Thus, the improvements of the themselves are considered scientific advances but the standard (GRS80) should not be changed.

When the information on the datum is obtained from positions within the orbit of the satellites (dynamic determination of the system), the coefficients of the gravitational potential (J2), as well as some constants (ω, speed of light, geocentric gravitational constant) are part of the datum definition since they are all calculated together.

An example of this last group is the World Geodetic System 1984 (WGS84) used by the GPS technique and obtained exclusively from the data of the GPS satellite constellation.

The values of its main parameters are:

a = 6378137 m

J2 = 108262,9983·10-8

GM = 3986004.418·108 m3/sg2

ω = 7293115·10-11 rd/sg

1/f = 298.257223563

The World Geodetic System 1984 (WGS84) uses the I.E.R.S. pole as the Z axis and the 0-meridian defined by the I.E.R.S. as the X axis. and the Y axis forming the right-handed triplet. Its origin coincides with the geocenter.

On a practical level, as can be deduced, the GRS80 and the WGS84 can be considered identical.

#### 2.1.3.2 Local geodetic reference systems. ED50

If $\Delta X \neq \Delta Y \neq \Delta Z \neq 0$ we are faced with a local datum. The local frame is defined by seven parameters (or, rather, 6 plus a condition): values for a and f (geometry of the ellipsoid), values of the deviations from the vertical ( $\xi$ , $\eta$ ) and the undulation of the geoid (distance between the reference ellipsoid and the geoid), these three parameters are used to obtain the orientation of the ellipsoid, the geodetic azimuth of a line and, as a condition, that the semi-minor axis of the ellipsoid and the mean axis of the earth's rotation are parallel. In addition, it is tried that the ellipsoid fits as much as possible to the area to be mapped, so that the reduction of observations is as simple as possible.

An example of this type of system is the ED-50 (European Datum of 1950), a system to which all Spanish cartography refers.

This system adopted the Hayford or International ellipsoid, introduced by the IUGG at its 1924 general assembly in Madrid, where a and f were obtained from astronomical and geodetic measurements in the United States.

a = 6378388

f = 1/297

Potsdam was adopted as a fundamental point, where the deviation from the vertical (angular difference between the geodetic and astronomical vertical) and the undulation of the geoid are known ($\xi$ = 3".36, $\eta$ = 1" .78, N = 0), so that the ellipsoid is oriented with respect to the Earth. It should be noted that setting the values of the deviation from the vertical ($\xi$, $\eta$) and

the value of the undulation of the geoid N at the fundamental point to orient the ellipsoid is equivalent to setting it from the X, Y, Z coordinates of its center with respect to the geocenter, figure 7.

ED50's accuracy ranges from a few meters in central Europe to more than 10 meters in the south, although its relative accuracy is much higher and more than sufficient for small- and medium-scale mapping surveys, so in 1968, the Army Geographical Service adopted it for its basic cartography 1/50000 and also the IGN in 1979.

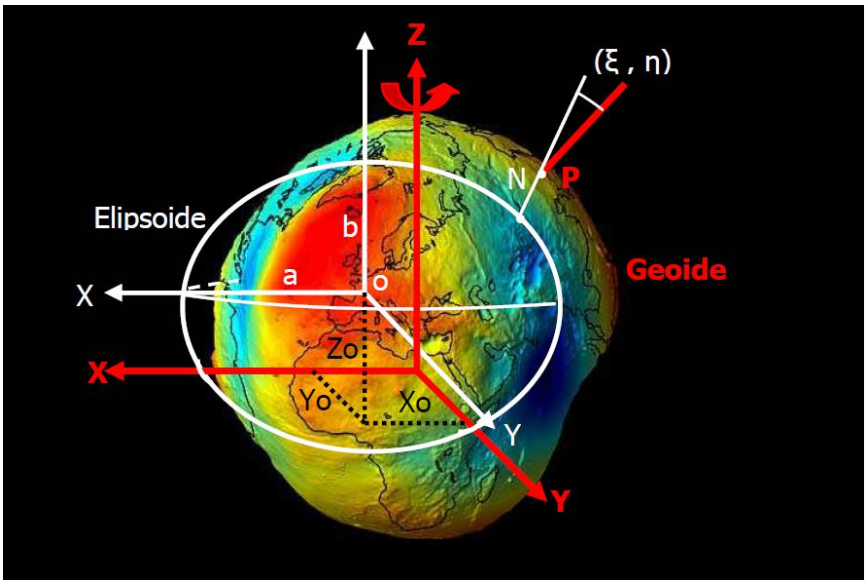


**Figure 7 Local geodetic system [4]**

### 2.1.4 International Terrestrial Reference Frame (ITRF)

The conventional international terrestrial reference system is materialized through the coordinates of a series of stations distributed throughout the world in that reference system, constituting the ITRF (International Terrestrial Reference Frame), established and maintained by the IERS.

Basically, the system that materializes is defined as geocentric (including the atmosphere and oceans), the basis for the scale is the meter (in the international system) and with the orientation of its axes as established by the BIH in 1984:

• Z axis: Middle pole determined by the IERS and called IERS Reference Pole (IRP) or Conventional Terrestrial Pole (CTP).

• X axis: Conventional Greenwich Meridian determined by the IERS and called IERS Reference Meridian (IRM) or Greenwich Mean Origin (GMO).

• Y axis: Forming a right-handed triplet with the previous axes on the conventional equator plane.

The frame is formed by Cartesian coordinates and speeds of a series of stations equipped with spatial observation techniques (VLBI, SLR, LLR, GPS since 1991 and DORIS since 1994), in figure 8 the stations for the ITRF2000 can be seen. If geodetic coordinates are desired, the use of the GRS80 ellipsoid is recommended. These coordinates implicitly define the origin, scale, and orientation of the X, Y, Z coordinate axes of the reference system.

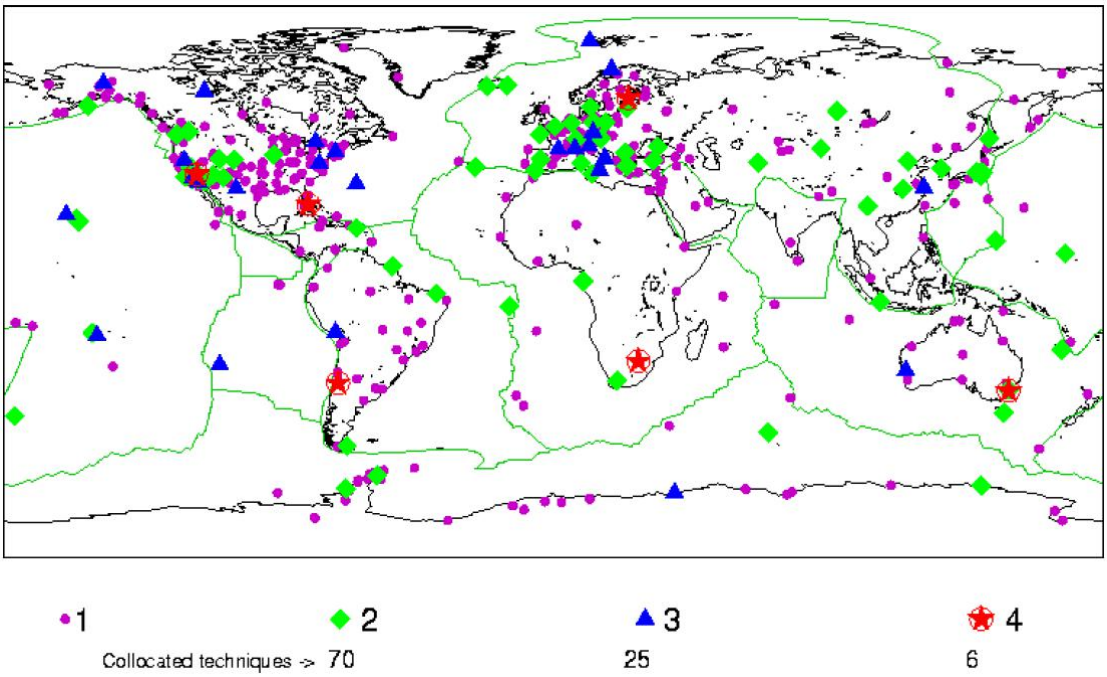


**Figure 8 Stations that make up the ITRF2000 symbolized according to the number of different spatial techniques they use. (www.researchgate.net)**

## 2.2 GNSS

The concept of GNSS is the generic standard term that encompasses Satellite Navigation Systems that provides geospatial positioning with global coverage, both autonomously and with augmentation systems. The beginnings date back to 1958, after the launch of Sputnik 1, launched on October 4, 1957 by the Soviet Union, it was the first artificial satellite in history to reach Earth orbit, a month later Sputnik is launched 2 and then,

in 1958, the first American Vanguard I satellite. In this way, the decade of the 60s meant a great commitment to navigation systems and that is how in 1964 the first satellites of the NAVSTAR constellation were launched in the United States. In 1969 with the Apollo 11 space mission, laser reflectors were placed on the Moon and that same year the first base was measured by Very Long Baseline Interferometry (VLBI). In the 1980s, the United States Department of Defense (DoD) developed GPS as a positioning and navigation system. Important advances are made in VLBI and Doppler Orbitography and Integrated Radio positioning by Satellite (DORIS) techniques. In the following years, the development of Spatial Geodesy focused its efforts on establishing the world geodetic system, determining geopotential models and measuring the Earth's gravity field. [17]

### 2.2.1 Land Use and Land Cover

Generally, Land use refers to how the land is used by people, while land cover refers to the physical and actual categories of land. The information and data of the both land use and land cover are often obtained from analysis of aerial and satellite imagery. Land cover signifies the biological and physical cover of the ground, whether it is artificial structures, vegetation, bare soil, water, or others [19]. Identification and mapping of land cover is important for the monitoring and the change detection studies, resource management and for future planning activities [20]. On the other hand, Land use has a more complicated aspect, because it involves principles management and social sciences and refers to the purpose the land serves, for example, habitat, recreation, agriculture, or other economic and social purposes.

## 2.3 GNSS Signal

The satellites that make up the navigation and positioning system have clocks or oscillators. These are atomic clocks for cesium, rubidium, and in some cases hydrogen. These clocks generate waves, called carriers, and all the information is supported on them. Atomic clocks maintain a stable and continuous time scale, they use the time pattern associated with International Atomic Time (TAI). On the other hand, GNSS receivers use quartz oscillators.

## 2.4 GNSS Observation

The concept of observables in satellite navigation refers to the ranges that are deduced

from the time measured between the signals received by the receiver (moment of reception) and the signals generated by the satellite (moment of emission). Unlike terrestrial electronic distance measurements, satellite navigation uses the "one-way concept" in which two clocks intervene, one on the satellite and the other on the receiver. Therefore, the ranges are skewed by satellite and receiver clock errors and are therefore denoted as pseudoranges. [18]. As mentioned, [17], there are three groups of GPS observables:

- Time observables, which will allow obtaining the pseudo-distances from the code.
- Phase difference observables.
- Observable Doppler.

The new signal structures for GPS, GLONASS, GALILEO and BDS allow to generate code and phase.

### 2.4.1 Pseudorange

As stated by [18] and as observed in figure 9, if we denote with $t^{sat}$ the time of emission of the signal referred to the reading of the satellite clock and with $t_{rec}$ the time of reception of the signal referring to the reading of the receiver clock, the errors of the clocks or biases with respect to a common time system can be estimated, for which they are called $t^{sat}$ and $t_{rec}$. On the other hand, the difference between the clock readings is equivalent to the time change $\Delta t$, which synchronizes the satellite and the reference signal during the code correlation procedure at the receiver, as shown in figure 10 and is expressed in equation (2,1).

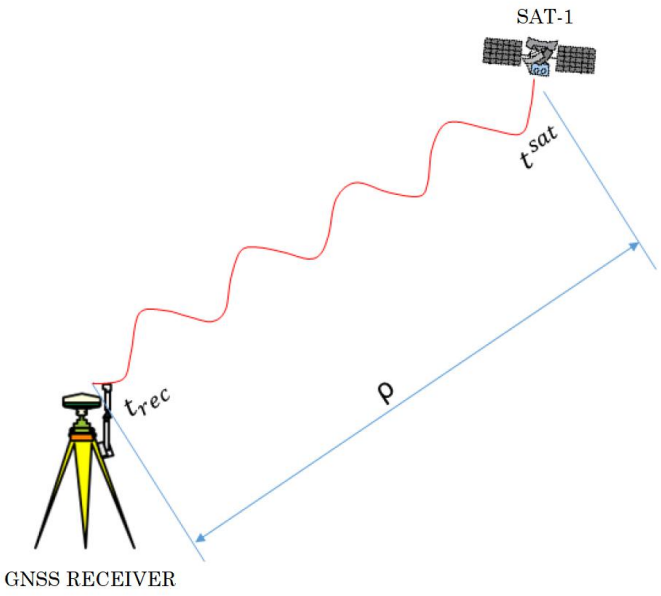


**Figure 9 Pseudorange signal [18]**

$$t_{rec} - t^{sat} = [t_{rec} + \delta_{rec}] - [t^{sat} + \delta^{sat}] = \Delta t + \Delta\delta \tag{2.1}$$

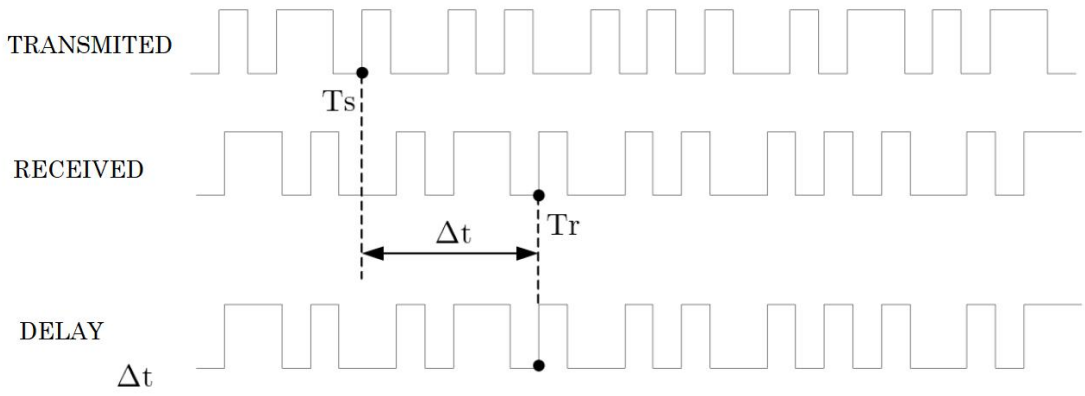


**Figure 10 Signal synchronization [18]**

Now, as indicated by [19], in equation (2.1), $t_{rec}$ and $t^{sat}$ are involved two different time systems but now on the right-hand side of this equation $t_{rec}$ and $t^{sat}$ are at the same time system common and where $\Delta t = t_{rec} - t^{sat}$ y $\Delta\delta = \delta_{rec} - \delta^{sat}$. The $\delta^{sat}$ bias of the satellite clock can be modeled if the respective information is transmitted accordingly by a polynomial with the coefficients that are transmitted in the navigation message. In such a way

that when multiplying the time interval of the expression $t_{rec} - t^{sat}$ of equation (2.1) that is affected by clock errors and by the speed of light, the code pseudorange expression is expressed in the equation (2,2).

$$R = c[t_{rec} - t^{sat}] = c\Delta t + c\Delta\delta = \rho + c\Delta\delta \tag{2.2}$$

On the other hand, as indicated [19], in practice, the clocks are not synchronized with each other, both the receiver clock and the satellite clock have a drift with respect to the system time and that together with others Errors make it impossible to accurately calculate the distances, in this way the pseudorange or code measure is calculated by default. Which in other words corresponds to the distance between the satellite's $t^{sat}$ epoch and the receiver's antenna position in the $t_{rec}$ epoch. However, reality is not limited only to this, since in addition to the problems mentioned, there are several errors that distort the signal when crossing the atmosphere, such as relativistic effects, delays, multipath error and others of less importance, which produce disturbances that they delay the signal. Therefore, the pseudorange is expressed as observed in equation (2.3).

$$R_i = \rho + c(\delta t_{rec} - \delta t^{sat}) + \Delta^{tropo} + \Delta^{iono} + \Delta_m + \varepsilon_i + \Delta_a^{sat} + \Delta_a^{rec} \tag{2.3}$$

Where:

$R_i$ = Pseudorange

$\rho$ = Is the geometric distance between the satellite and the antenna phase center (APC) of the receiver at the time of transmission and reception respectively.

$c$ = speed of light

$\delta t_{rec}$ = Receiver state clock

$\delta t^{sat}$ = Satellite state clock

$\Delta^{tropo}$ = It is the delay in the signal caused by passing through the troposphere layer

$\Delta^{iono}$ = It is the ionospheric effect produced by the signal passing through the ionosphere layer, and given its dispersive nature, the term will depend on the frequency.

$\Delta_m$ = Errors due to the multipath effect of the observable code

$\varepsilon_i$ = Errors due to unmodeled effects that contribute to the observation noise

$\Delta_a^{sat}$ = Satellite antenna center correction

$\Delta_a^{rec}$ = Receiver antenna correction

### 2.4.2 Phase measurements

As stated by [20], it is affirmed that the synchronization between the carrier of the received signal and the replica generated in reception allows obtaining a measure of the phase of the carrier. This phase measurement can also be used to estimate the satellite and receiver distance. Therefore, the distance measure can be calculated by measuring the integer $N$ of wavelengths $\lambda$ and the non-integer part $\varphi$, as seen in equation (2.4) and in figure 11.

$$D = \lambda(N + \varphi) \tag{2.4}$$

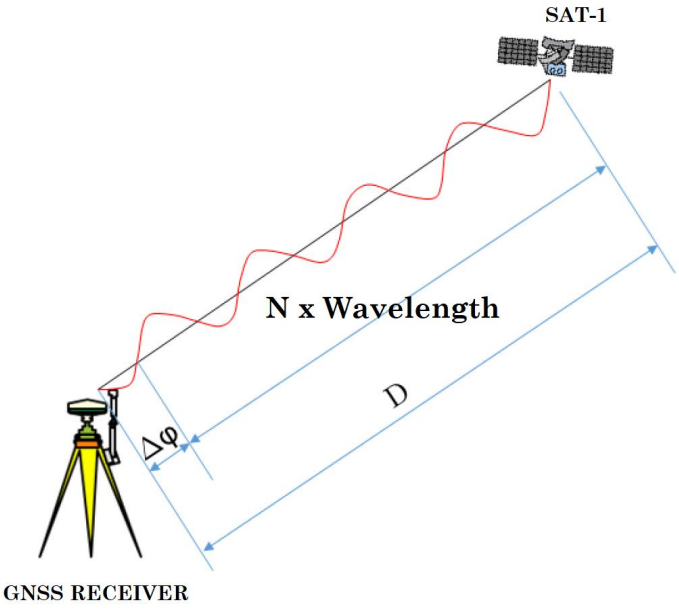


**Figure 11 Phase measurements [18]**

This simple idea is not easy to carry out given the difficulty of determining $N$, and this problem is called the determination of ambiguities. The phase measurement is usually expressed in carrier cycles. So, this distance will be equal to the integer number of carrier cycles $N$ elapsed since the signal left the satellite until it reaches the receiver, plus the fraction of the cycle measured. The phase observable is the difference between the phase of the carrier received from the satellite and the phase generated internally by the oscillator of the receiver. These phase measurements are recorded at equal time intervals from the receiver, and do not take into account the number of waves between the receiver and the satellite, but the observable phase variations over time are correlated with changes in topocentric distance [17].

In abbreviated form, the general equation of the phase observable can be expressed as follows, see equation (2.5). [19]

$$\phi = \rho + c\Delta\delta + \lambda N + \Delta^{tropo} - \Delta^{iono} + \Delta_m + \varepsilon_i \tag{2.5}$$

The number of cycles between satellite and receiver depends on the phase generated by

the oscillators. As in pseudorange, there are clock errors, and also in its route it suffers the effects of delay or advance of the signal when crossing the atmosphere, and other errors such as multipath. Therefore, in equation (2.6), the general expression in linear units is observed:

$$\phi_i = \rho + c(\delta t_{rec} - \delta t^{sat}) + \lambda N + \Delta^{tropo} - \Delta^{iono} + \Delta_m + \varepsilon_i + \lambda_i \omega + \Delta_{cf}^{sat} + \Delta_{cf}^{rec} + \lambda_\phi^{sat} + \lambda_\phi^{rec} \quad (2.6)$$

Where:

$\rho$ = Is the geometric distance between the satellite and the antenna phase center (APC) of the receiver at the time of transmission and reception respectively.

$c$ = speed of light

$\delta t_{rec}$ = Receiver state clock

$\delta t^{sat}$ = Satellite state clock

$\lambda N$ = Represents ambiguity

$\Delta^{tropo}$ = It is the delay in the signal caused by passing through the troposphere layer

$\Delta^{iono}$ = It is the ionospheric effect produced by the signal passing through the ionosphere layer, and given its dispersive nature, the term will depend on the frequency.

$\Delta_m$ = Errors due to the multipath effect of the observable code

$\varepsilon_i$ = Errors due to unmodeled effects that contribute to the observation noise

$\lambda_i \omega$ = Windup effect of circular polarization of the electromagnetic signal with

$\Delta_{cf}^{sat}$ = Satellite antenna center correction

$\Delta_{cf}^{rec}$ = Receiver antenna correction

$\lambda_\phi^{sat}$ = Phase bias on satellite

$\lambda_\phi^{rec}$ = Phase bias on receiver

Finally, in equation (2.7), it is expressed in cycle units:

$$\phi = \frac{\rho}{\lambda} + \frac{c\Delta\delta}{\lambda} + N + \frac{\Delta^{tropo}}{\lambda} - \frac{\Delta^{iono}}{\lambda} + \Delta_m + \varepsilon_p \tag{2.7}$$

# 3 Mathematical Model

The research methodology is the plan followed in the study to reach the objectives of the study, in which we explained the strategy that we followed in terms of collecting various days of data, and the methods of processing and analyzing them.

## 3.1 Precise point position (PPP) method

Precise point position (PPP) [21] is a one common positioning method which are applying in static or kinematic observation by using a single receiver and also using GNSS CORS station observation data, satellite orbit and satellite clock products to find out best precise accuracy for user. PPP method provide to all user a very high-level millimeter or centimeter precise positioning accuracy. Lot of researchers are using this method for their GNSS research and solved problem. In all over the world there is software used for PPP method. Using a single receiver, it can be estimate position, velocity, troposphere delay, ionosphere delay, satellite determination etc. PPP method have lot of application such as water vapor monitoring, weather monitoring, lot of commercial and agricultural sectors.

### 3.1.1 PPP processing technique

The perfect product of GPS satellite orbit and real-time availability has been activated the development of a global positioning system is known as the specific Precise Point Positioning (PPP). The pseudorange and carrier phase observations are using single GPS receiver to the position accuracy millimeter to centimeter level. So, in GNSS positioning system community the importance of PPP is significantly expected [22]. PPP are used in many sections for example monitoring position movement to maintain international reference bases by filling the Global Positioning System (GPS). The accuracy of PPP method has increased due to the use of accurate clock and satellite products. The PPP operating system all PPP algorithm such as Kalman filter model, Functional Model, and also PPP stochastic model are developed using data collected by dual frequency GPS receiver. Using technological errors for example tropospheric error and error data coordination to measure all PPP models' errors is believed to improve the accuracy of the position. Permanent Filter Safety is also used

for evaluating state data as information on different positions and diversity. For verification, we compare the all results to more at GNSS CORS data observation in International Service Center (IGS) Analysis. Thus, the average position error is around the millimeters level in the east-north-up direction.

### 3.1.2 PPP functional models

The functional model is one kind of precise positioning technique which represent a clear relationship between unknown and the observations [23]. The functional model can estimate GPS receiver and clock biases or many GPS biases positioning by using double differencing (DD) technique. Therefore, on GPS precise positioning mode the functional model is depends on the use of ionosphere-free linear combination in GPS observation. The following functional model equation given below:

$$S(l_i) = \xi + \partial_{obs} + c(\partial T) - c(\partial t) + \partial_{ino(l_i)} + \partial_{trop} + \partial^{r}_{hd(S(l_i))} - \partial^{s}_{hd(S(l_i))} + \partial_{muti(S(l_i))} + \partial_{noise(S(l_i))} \quad (3.1)$$

$$\Psi(l_i) = \xi + \partial_{obs} + c(\partial T) - c(\partial t) - \partial_{ino(l_i)} + \partial_{trop} - \varphi_{l_i}\vartheta_{l_i} + \partial^{r}_{hd(\Psi(l_i))} - \partial^{s}_{hd(\Psi(l_i))} + \partial_{muti(\Psi(l_i))} + \partial_{noise(\Psi(l_i))} \quad (3.2)$$

$$S_{ionofree} = \frac{F_1^2 S_1 - F_2^2 S_1}{F_1^2 - S_2^2} \quad (3.3)$$

$$= \xi + \partial_{obs} + c(\partial T) - c(\partial t) + \partial_{trop} + \partial^{r}_{hd(S_{ionofree})} - \partial^{s}_{hd(S_{ionofree})} + \partial_{muti(S(l_i))} + \partial_{noise(S_{ionofree})} \quad (3.4)$$

$$\Psi_{ionofree} = \frac{F_1^2\Psi_1 - F_2^2\Psi_2}{F_1^2 - S_2^2} = \xi + \partial_{obs} + c(\partial T) - c(\partial t) + \partial_{trop} - \varphi_{l_{ionofree}}\vartheta_{ionofree} + \partial^{r}_{hd(\Psi(l_i))} - \partial^{s}_{hd(\Psi(l_i))} + \partial_{muti(\Psi(l_i))} - \partial_{noise(\Psi(l_i))} \quad (3.5)$$

Where,

$S(l_i)$ = Measurement of pseudorange on $li$ frequency, in meter unit

$\Psi(l_i)$ = Measurement of carrier-phase on $li$ frequency, in meter unit

$\xi$ = Receiver and satellite distance, unit is meter

$c$ = Speed of light, unit is meter/second

$\partial T$ = Error (satellite clock), unit is second

$\partial t$ = Error (receiver clock), unit is second

$\partial_{ino(l_i)}$ = Ionosphere delay in frequency $li$, unit is meter

$\partial_{trop}$ = Zenith troposphere delay, unit is meter

$\partial^{r}_{hd(S(l_i))}$ = In $li$ frequency pseudorange measurement it is delay of receiver hardware bias, unit is meter

$\partial^{s}_{hd(S(l_i))}$ = In $li$ frequency pseudorange measurement it is delay of satellite hardware bias, unit is meter

$\partial_{muti(S(l_i))}$ = Multipath error of $li$ frequency pseudorange measurement, unit is meter

$\partial_{noise(S(l_i))}$ = Noise error of $li$ frequency pseudorange measurement, unit is meter

$\varphi_{l_i}$ = weave length of $li$ frequency carrier-phase measurement, in cycle unit

$\vartheta_{l_i}$ = Ambiguity of $li$ frequency carrier-phase measurement, in cycle unit

$S_{ionofree}$ = Ionosphere free measurement of pseudorange on $li$ frequency, in meter unit

$\Psi_{ionofree}$ = Ionosphere free measurement of carrier-phase on $li$ frequency, in meter unit

$\varphi_{l_{ionofree}}$ = Ionosphere free wave length of $li$ frequency carrier-phase measurement, in cycle unit

$\vartheta_{ionofree}$ = Ionosphere free Noise error of $li$ frequency pseudorange measurement, unit is meter

### 3.1.3 Least square estimation

The least-squares estimation method is commonly used in GPS observation data processing [24]. Last square method is a well-defined and useful rule for estimating parameters and also quality control of assessing by GPS observation data processing are using mathematical model [25]. The core stations are static, Last square estimation (LS) method is more suitable for static solution. Filter method, e.g., Kalman filtering, might be suitable for kinematic solution. In present GNSS research LS method is using by preudorange and carrier

phase measurements to find out accurate precise point positioning also using dual frequency GNSS receiver. GPS receiver positioning individually can happen error in preudorange or carrier phase applications so by using preudorange measurement data we get very less precise positioning with more movement. But again, using carrier phase data we get better precise positioning with displacement but data accuracy is much high.

The following equation of last square estimation method is [26]:

$$V = AX - L; P \tag{3.6}$$

Where,

$L$ = n dimensional of observation vector in this system

$X$ = is m dimensional parameter of vector which is usually unknown parameter in the system

$V$ = is n dimensional residual vector of the system

$A$ = is n by m dimensional coefficient of matrix of the estimation

$P$ = is n by n dimensional symmetric matrix in this estimation and it is also weight matrix

The last square estimation method equation error can be solved by the following equation:

$$V^T PV = \text{minimum of value} \tag{3.7}$$

Where,

$V^T$ = is transpose vector of n dimensional of residual vector matrix

$$A^T PV = 0 \tag{3.8}$$

Where,

$A^T$ = is transpose vector of n by m dimensional coefficient of this estimation matrix

Compare the equation of (3.6) and (3.7) we get from the equation:

$$\begin{aligned} &A^T P(AX - L) = 0 \\ &A^T PAX - A^T PL = 0 \\ &A^T PAX = A^T PL \\ &X = (A^T PA)^{-1} A^T PL \end{aligned} \tag{3.9}$$

Now we have to know as,

$$M = A^T PA \tag{3.10}$$

And $$Q_X = (A^T PA)^{-1} \tag{3.11}$$

Hare, $M$, and $QX$ are respectably known as normal and cofactors matrix in the equation

$$\sum X = Q_X \sigma_0^2 \tag{3.12}$$

Hare $\Sigma X$= is covariance matrix of this equation and m dimensional parameter and also $\sigma_0$ is standard division and the complete equation of this last square estimation is following:

$$\sigma_0 = \sqrt{\frac{V^T PV}{n-m}} \quad \text{(Hare n is greater than m)} \tag{3.13}$$

Hare the other equation is

$$V_k = A_k X_k - L_k; P_k \tag{3.14}$$

$V_k =$ $nk$ dimensional residual matrix epoch time is $k$

$A_k =$ $nk$ by m dimensional coefficient of matrix of epoch is $k$

$X_k =$ $mk$ dimensional unknown parameter vector epoch is $k$

$L_k =$ $nk$ dimensional observation vector and epoch time is $k$

$P_k =$ $nk$ $by$ $nk$ dimensional symmetric matric which $k$ is epoch

$$V_k^T P_k V_k + (X_k - X_{k-1})^T P_{X_{k-1}} (X_k - X_{k-1}) = \text{minimum of value} \tag{3.15}$$

Solving this (3.14) using (3.15) equation is following below:

$$A_k^T P_k V_k + P_{X_{k-1}} (X_k - X_{k-1}) = 0 \tag{3.16}$$

Compare (3.14) and (3.16) equation we get from the following below,

$$(A_k^T P_k A_k + P_{X_{k-1}}) X_k - (A_k^T P_k L_k + P_{X_{K-1}} X_{k-1}) = 0 \tag{3.17}$$

So least squares solution is the following below from equation (3.18)

$$X_K = (A_k^T P_k A_k + P_{X_{k-1}})^T (A_k^T P_k L_k + P_{X_{K-1}} X_{k-1}) \tag{3.18}$$

$$P_{X_k} = A_k^T P_k A_k + P_{X_{k-1}} \tag{3.19}$$

$$X_K = P_{X_k}^{-1}(A_k^T P_k L_k + P_{X_{k-1}} X_{k-1}) \tag{3.20}$$

$$Q_{X_k} = P_{X_k}^{-1} = (A_k^T P_k A_k + P_{X_{k-1}})^{-1} \tag{.21}$$

So, equation (3.20) is the solution of least squares estimation

$$\begin{aligned} X_1 &= P_{X_1}^{-1} A_1^T L_1 \\ X_2 &= P_{X_2}^{-1}(A_2^T P_2 L_2 + P_{X_1} X_1) \\ &\cdots\cdots \\ X_k &= P_{X_{k-1}}^{-1}(A_k^T P_k L_k + P_{X_{k-1}} X_{k-1}) \end{aligned} \tag{3.22}$$

$$\begin{aligned} P_{X_1} &= A_1^T P_1 A_1 \\ P_{X_2} &= P_{X_1} + A_2^T P_2 A_2 \\ &\cdots\cdots \\ P_{X_k} &= P_{X_{k-1}} + A_k^T P_k A_k \end{aligned} \tag{3.23}$$

Hare, $\Sigma Xk=$ is covariance matrix of this equation and $mk$ dimensional parameter and also $\sigma 0k$ is standard division and the complete equation of this last square estimation is following:

$$\sum X_k = Q_X \sigma_{0_k}^2 = P_{X_k}^{-1} \sigma_{0_k}^2 \tag{3.24}$$

$$\sigma_{0_k} = \sqrt{\frac{V_k^T P_k V_k + (X_k - X_{k-1})^T P_{X_{k-1}} (X_k - X_{k-1})}{n_k}} \tag{3.25}$$

Where, in this last square estimation observation number is $nk$ and epoch is $k$

## 3.2 Error Sources of PPP

### 3.2.1 Satellite Clock and receiver clock

Satellite clock error is one of the systematic errors in GPS positioning because it is transmitted the navigation massage. And the receiver clock error is measurement from difference receiver clock time and also GPS time. The receiver clock basis error is unknown and it also assumed together with the receiver's location and receiver velocity. So, both of satellite and receiver error can be estimated by using appropriate linear combination of differential GPS [27].

In GNSS satellite clocks measurement are very accurate. But a small error of the satellite clock which show a significant error in GNSS receiver positioning system. For

example, in GNSS satellite clocks 20 nanoseconds error require can happened 6-meter positioning error in GNSS receiver [28]. Receiver ground control system of GNSS is use more accurate clock and also monitoring satellite clock. To get a good a precise positioning the ground control GNSS receiver to recoup for GNSS satellite clock error. PPP service system also provide in online satellite clock information to solve the satellite clock error. PPP system or Space Based Argumentation System (SBAS) also correction satellite clock error for precise positioning. There is another way is configuration of RTK receiver to make amends for satellite clock error.

### 3.2.2 Satellite orbit

GNSS satellite travels on specific orbit, like satellite clocks. Ground control system of GNSS is always monitoring this satellite orbit error. Satellite orbit is another significance error GNSS positioning system tike satellite clock error. When GNSS satellite orbit changes his moving way then ground control system send massage for correction, so satellite orbit updated this information. Ground control system which are send to satellite for correction if any effects in GNSS positioning system like ±2.5 meters positioning error can happen. To solve the satellite orbit error one way is precise ephemeris information is upload from PPP service and another way to solve configuration for RTK receiver.

### 3.2.3 Ionosphere delay.

An atmospheric layer between 80km to 600km of ionosphere. This level is said to electric partials level. This electric partial means ions. And also, these ions can delay satellite signals and create a usually ±5 meters positioning error. But at that time ionosphere activity may be larger. Ionosphere delay depends on solar activates, season, day, time and location. So, this delay is affected to calculate positions. There is another reason passing signal of radio frequency in ionosphere is causes ionosphere delay. GNSS precise receiver $L1$ and $L2$ signal and signals are measurement error. GNSS receiver can determine the ionosphere delay and remove this error and calculate the positions. Also, ionosphere model can be used to remove the error.

### 3.2.4 Troposphere delay

In earth's atmosphere surface up to 50 km layer is the troposphere. The ionosphere

delay and troposphere delay are dependent each other. It is not possible to remove the troposphere error by using dual frequency GPS receivers. Satellite elevation angle and the atmosphere condition is effects of GPS signal to create the troposphere error. The tropospheric delay is divided into two component they are dry and wet. In total atmospheric conditions about 90% is dry component which is depends on density of gas molecules. The wet component is displacement due to electrons and water molecules. Water vapor is the reason for wet atmosphere and difficult to model it. The effects of the troposphere are 2 m delay to 25 m with elevation angle is 5 degrees. For short baselines using DD (double differencing) to estimate the troposphere errors and DD model is the part of estimation of this process. In my research the last part is also about zenith troposphere delay (ZTD) analysis by using my countries GNSS CORS station long time observation raw data. The analysis can deal with a new concept and idea for me about troposphere affects in Peru.

### 3.2.5 Satellite antenna phase center offset and variation

The phase center is significant for GNSS satellite and receiver antenna. The phase centers are measured distance between on ground GNSS receiver and GNSS satellite and its serves as the last point. So, phase center offset (PCO) and phase center variation (PCV) value are more important because they exact position are create modeled for experiment and calculation. The center mass of satellite, reference point of receiver antenna and mean value of phase center all are described by POC. And otherwise, to get accurate actual phase center position PCV value is more important because it provide corrections foe zenith [29]. Mass of satellite center is comparing to the GPS orbit. The GPS observation mention antennas phase center and the antenna phase offset must be known. POC measurement is so difficult because phase center is an electronic point not to be mechanical. In hare it’s considered an error in Z direction [30]. Which is written by the following below.

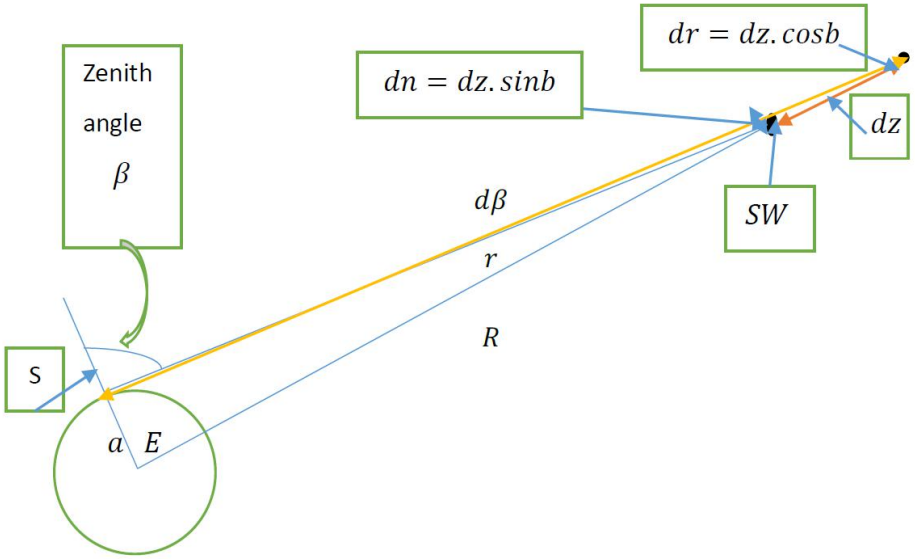


**Figure 12 GPS error of z-direction effects**

Where,

$R$=Radius of satellite

$a$=Radius of earth

$r$=satellite of receiver distance

$b$=Observation angle which is satellite to receiver and receiver to geometer vector and it consider to zero station height and ZPD (zenith path delay) so this is the error of GPS positioning [30].

GPS antenna is the most important element for GPS satellite and GPS receiver because it always connecting each other. Antenna are receiving signal from satellite and it converts into electronic component. On the other hand, in GPS positioning accurate antenna PCO and PCV are another most critical factor. Some GPS user use very simple offset value which are not enough value for precise positioning. Again, in GPS precise positioning other GPS user avoid phase center correction factors. So, both are creating error for PPP method and coordinate results are not very precise specially height direction [31].

### 3.2.6 Earth tide

The earth tides depend on motion of solid earth and its gravitational ability, inspired by the external tides force. The evolution of fossils has the important paleontology, there

experiment can provide lot of information about the earth tides, from some of the measurements the model can be used to remove tidal variations and also used for trial effects [32]. GPS technology is a very useful tools for crustal movement and also geodynamics science. Using GPS system to monitor forecasting area of high earthquake and crustal movement. We also consider the satellites error, receiver's error, as well as take into tectonic deformation effects, gravity of atmosphere, ocean and pole tide etc. For tectonic distortion and get accurate value so this error should be analyzed and considered. Solid earth tide which is the variable distortion of a period time due to the gravitational effects of sun and the moon [33]. And the moon is most dominant.

The following equation from [34], [33] is solid earth model

$$\Delta\vec{r} = \sum_{j=2}^{3} \frac{GM_j}{GM} \frac{r^4}{R_j^3} \left\{ \left[3l_2(\bar{R}_j * \bar{r})\right] R_j + \left[ (\frac{h_2}{2} - l_2)(R_j * \hat{r})^2 - \frac{h_2}{2} \right] \hat{r} \right\} + [-0.025 * \sin\phi * \cos\phi * \sin(\theta_g + \lambda)] * \hat{r} \quad (3.26)$$

Where,

$GM$= Earth's parameter of gravitation

$GMj$= Moon and sun parameter of gravitation ($j$=2, $moon$: $j$=3, $sun$)

$R$=Stations geocentric state vectors

$Rj$=Moon and sun geographic unit state vector ($j$=2, $moon$: $j$=3, $sun$)

$\hat{r}$= Stations state vectors of the geocentric unit

$\hat{R}j$= Moon and sun Station's state vectors of the geocentric unit ($j$=2, $moon$: $j$=3, $sun$)

$l2$= Second degree of nominal love number

$h2$= Dimensionless of nominal Shida number

$\phi$=Latitude of site stations

$\lambda$= Longitude of site stations

$\Theta^g$=Mean of Greenwich Time

### 3.2.7 PPP algorithm

PPP algorithm are widely use in different application. For the accurate positioning measurement PPP are using dual-frequency GPS receiver for determine to the positioning accuracy level is centimeter to decimeter. We know, ionosphere effects are another important

error in GPS positioning measurement. Dual frequency GPS receiver can eliminate the ionosphere error. This requirement of dual frequency receiver's importance. On the other hands most of GPS receiver use single frequency because it is beneficial for PPP to investigate the method and algorithm [35]. The following PPP algorithm observation equation is given below [36]

$$P^s_{r,f,k} = g^s_{r,k} + \gamma f \tau^s_{r,i,k} + c_0 d^s_{r,f,k} + \underline{\varepsilon^s_{r,j}} \tag{3.27}$$

$$\Phi^s_{r,f,k} = g^s_{r,k} - + \gamma f \tau^s_{r,i,k} + \lambda f A^s_{r,j} + c_0 \delta^s_{r,f,k} + \underline{\varepsilon^s_{r,j}} \tag{3.28}$$

where,

$P$=Random variable of Pseudorange observation

Φ= Random variable of carrier phase observation

$r$=Index of receiver

$f$= Index of frequency

$k$=Measurement of time epoch

$g$=Geometric range

$s$= Index of satellite

$\gamma$=Dispersion factor of ionosphere

$\tau$=Travel time of signal

$c0$=Speed of light (vacuum)

$d$=Systematic delay

$A$=Ambiguity of carrier phase

$\epsilon$=Error of code measurement

$\delta$=Carrier phase measurement

$a$= Linear combination of frequency

$b$= Linear combination of frequency

#### 3.2.7.1 Single frequency algorithms

The first order ionosphere delay wiped out code-phase-carrier (CPC) combination [37]. The ionosphere-free code observation and phase observation are using single frequency GPS receiver in GNSS precise positioning can defined the following equation [36]:

$$\underline{CPC}^{s}_{r,f,k} = \frac{1}{2}(\underline{P}^{s}_{r,f,k} + \underline{\Phi}^{s}_{r,f,k}) \tag{3.29}$$

From the equation (3.27) and (3.28) we get,

$$\underline{CPC}^{s}_{r,f,k} = g^{s}_{r,k} + \frac{1}{2}A^{s}_{r,f} + \frac{1}{2}c_0(d^{s}_{r,f,k} + \delta^{s}_{r,f,k}) + \frac{1}{2}(\underline{\varepsilon}^{s}_{r,j} + \underline{\varepsilon}^{s}_{r,j}) \tag{3.30}$$

### 3.2.7.2 Dual frequency algorithms

The ionosphere free linear combination is very costly and very noisy and create measurement error for receiver and multipath. In GNSS precise positioning method are use two different algorithms for ionosphere-free linear combinations such as ionosphere-free linear combinations of carrier phase and ionosphere-free linear combinations of pseudorange observations. The primary convergence makes a difference for pseudorange observations but final solution is depending on carrier phase observations. The ionosphere free linear combination of dual frequency equations is written the following method [36]:

$$\underline{P}^{s}_{r,LC,k} = a\underline{P}^{s}_{r,a,k} + b\underline{\Phi}^{s}_{r,b,k} \tag{3.31}$$

$$\underline{\Phi}^{s}_{r,LC,k} = a\underline{\Phi}^{s}_{r,a,k} + b\underline{\Phi}^{s}_{r,b,k} \tag{3.32}$$

From the equation (3.27) and (3.28) and using $fi{=}kif0$ we get,

$$\underline{P}^{s}_{r,LC,k} = (a+b)g^{s}_{r,k} + (\frac{a}{k_a^2} + \frac{b}{k_b^2})\tau^{s}_{r,0,k} + c_0(ad^{s}_{r,a,k} + bd^{s}_{r,b,k}) + (a\underline{\varepsilon}^{s}_{r,ak} + b\underline{\varepsilon}^{s}_{r,bk}) \tag{3.33}$$

$$\underline{\Phi}^{s}_{r,LC,k} = (a+b)g^{s}_{r,k} - (\frac{a}{k_a^2} + \frac{b}{k_b^2})\tau^{s}_{r,0,k} + \frac{c_0}{f_0}(\frac{a}{k_a}A^{s}_{r,a} + \frac{b}{k_b}A^{s}_{r,b}) + c_0(a\underline{\delta}^{s}_{r,ak} + b\underline{\delta}^{s}_{r,bk}) + (a\underline{\varepsilon}^{s}_{r,ak} + b\underline{\varepsilon}^{s}_{r,bk}) \tag{3.34}$$

Now,
$$a = \frac{k_a^2}{k_a^2 - k_b^2} = \frac{\gamma b}{\gamma b - \gamma a}$$
$$b = \frac{k_b^2}{k_a^2 - k_b^2} = \frac{-\gamma b}{\gamma b - \gamma a} \tag{3.35}$$

From equation (3.33) and (3.34) is ionosphere-free linear combinations as writing the following equation:

$$\underline{P}^{s}_{r,IF,k} = g^{s}_{r,k} + \frac{c_0}{k_a^2 - k_b^2}(k_a^2 d^{s}_{r,a,k} - k_b^2 d^{s}_{r,b,k})\tau^{s}_{r,0,k} + \frac{1}{k_a^2 - k_b^2}(k_a^2 \underline{\varepsilon}^{s}_{r,ak} - k_b^2 \underline{\varepsilon}^{s}_{r,bk}) \tag{3.36}$$

$$\Phi^{s}_{r,LC,k} = g^{s}_{r,k} + \frac{c_0}{(k_a - k_b)f_0}(k_a A^{s}_{r,a} - \frac{b}{k_b} k_b A^{s}_{r,b}) + \frac{c_0}{k_a^2 - k_b^2}(k_a^2 \delta^{s}_{r,ak} - k_b^2 \delta^{s}_{r,bk}) + \frac{1}{k_a^2 - k_b^2}(k_a^2 \varepsilon^{s}_{r,ak} + k_b^2 \varepsilon^{s}_{r,bk}) \tag{3.37}$$

# 4 Program

## 4.1 Data collection

Peru has 69 GNSS receivers installed along its territory, these track precise positioning data 24 hours per day and 365 days a year, figure 13.


**Figure 13 Location GNSS receivers, operating radius 100 Km**

With the data obtained from the GNSS receivers, it is possible to measure the variation of the position of stations after a tectonic event [2]; as is the case of the seismic event that occurred on May 26, 2019 at 02 hours - 41 minutes (Local time) [3] where there were considerable movements in the nearby stations of the epicenter, whose hypocentral

characteristics are shown in the following table:

**Table 1 Hypocentral characteristics earthquake**

| Feature | Magnitude | Comments |
|---|---|---|
| Latitude | -05.74° | --- |
| Longitude | -75.55° | --- |
| Depth | 135 Km | Intermediate focus event |
| Magnitude | 8 Mw | Magnitude |
| Reference | 60 Km South of Lagunas | Amazonas state |
| Maximum intensity | VII Lagunas Yurimaguas | Modified Mercalli scale |
| Date (UTC) | 26/05/2019 | Universal Time Coordinate |
| Start Time (UTC) | 07h 41m | Universal Time Coordinate |

The data was processed with scientific software PANDA software, obtained the coordinates before and after the earthquake.

For my research I used 14 GNSS stations surrounding the earthquake, and processed data to know the displacement of these GNSS stations.

Data was collected one week before and after earthquake, accounting 15 days for processing data day per day, data was collected from receivers as raw data, and then storage in memory hard of my institution, whole GNSS stations are TRIMBLE, and the first day data collected was since May 19 (139 JD) until June 2 (153 JD) of 2019, each data was collected day per day, each day are 24 hours, and 5 seg of recording interval.

GNSS data was extract from receiver, then putted in a directory's day per day, each directory day contain 14 GNSS stations, data origin is in format raw, *.T01 and *.T02 (Fig. 1.1) and is necessary get a program for convert these data in RINEX format.

Data is available per 24 hours each one and 5 sec interval epoch, in the table 2 show data available per stations and days, "x" mean data completed and, red "x" mean data completed seismic data day and "0" mean data unavailable, according data unavailable was

because GNSS receiver didn't recording for that day due electricity problems

**Table 2 Data available per stations and days**

| / | 139 | 140 | 141 | 142 | 143 | 144 | 145 | 146 | 147 | 148 | 149 | 150 | 151 | 152 | 153 |
|---|---|---|---|---|---|---|---|---|---|---|---|---|---|---|---|
| **AM01** | X | X | X | X | X | X | X | X | X | X | X | X | X | X | X |
| **AM03** | X | X | X | X | X | X | X | X | X | X | X | X | X | X | X |
| **AM05** | X | X | X | X | X | X | X | X | X | X | X | X | X | X | X |
| **CJ02** | X | X | X | X | X | X | X | X | X | X | X | X | X | X | X |
| **HC03** | X | X | X | X | X | X | X | X | X | X | X | X | X | X | X |
| **LB01** | X | X | X | X | X | X | X | X | X | X | X | X | X | X | X |
| **LR01** | X | X | X | X | X | X | X | X | X | X | X | X | X | X | X |
| **LR02** | X | X | X | X | X | X | X | X | X | X | X | X | X | X | X |
| **LR03** | X | X | X | X | X | X | X | X | X | X | X | X | X | X | X |
| **LR06** | X | X | X | X | X | X | X | X | X | X | X | X | X | X | X |
| **LR07** | X | X | X | X | X | X | X | X | X | X | X | X | X | X | X |
| **SM01** | X | X | X | X | X | X | X | X | X | X | X | X | X | X | X |
| **SM02** | X | X | X | X | X | X | X | X | X | X | X | X | X | X | X |
| **UC01** | X | X | X | X | X | X | X | X | X | X | X | X | X | X | X |

## 4.2 Observation data information

The GNSS data observation format was RINEX 2.11, and other important data used navigation, orbit and clock file. Navigation and orbit file was collected from IGS. RECEIVER INDEPENDENT EXCHANGE (RINEX) is developed for Astronomical Institute of the University of Berne for Global Positioning System (GPS) data to exchange for everyone all over the word [a]. There are many versions in RINEX format, for example: RINEX 1, RINEX 2 is two sub version, in the rinex 2.10 and RINEX 2.11 only contains GPS data.

```
     2.11           OBSERVATION DATA    M (MIXED)           RINEX VERSION / TYPE
teqc  2019Feb25                        20210406 21:12:44UTCPGM / RUN BY / DATE
Linux2.6.32-573.12.1.el6.x86_64|x86_64|gcc|Win64-MinGW64|=+ COMMENT
  0.0750      (antenna height)                                 COMMENT
  -3.90725109 (latitude)                                       COMMENT
 -70.51591094 (longitude)                                      COMMENT
0096.365      (elevation)                                      COMMENT
BIT 2 OF LLI FLAGS DATA COLLECTED UNDER A/S CONDITION          COMMENT
LR05 (COGO code)                                               COMMENT
LR05                                                           MARKER NAME
LR05                                                           MARKER NUMBER
DPG                 IGN-PERU                                   OBSERVER / AGENCY
5742R51288          TRIMBLE NETR9       5.22                   REC # / TYPE / VERS
51000419            TRM115000.00    TZGD                       ANT # / TYPE
  2122517.1616 -5999098.4711  -431720.1508                     APPROX POSITION XYZ
       0.0750        0.0000        0.0000                     ANTENNA: DELTA H/E/N
    1     1                                                    WAVELENGTH FACT L1/2
    7    L1    L2    C1    P1    P2    S1    S2               # / TYPES OF OBSERV
    5.0000                                                     INTERVAL
   18                                                          LEAP SECONDS
Forced Modulo Decimation to 5 seconds                          COMMENT
 SNR is mapped to RINEX snr flag value [0-9]                   COMMENT
  L1 & L2: min(max(int(snr_dBHz/6), 0), 9)                     COMMENT
  2021     2    27     0     0    0.0000000     GPS           TIME OF FIRST OBS
                                                               END OF HEADER
 21  2 27  0  0  0.0000000  0 16G03G28G17G09G06G07R09R12R22R07G30R08
                              G19G14R10G02
 124657372.895 6  97135605.99045  23721503.859                    23721508.816
        40.700          34.800
 113219521.892 7  88222961.85245  21544934.492                    21544934.375
        45.800          33.700
 127683146.677 6  99493407.30145  24297283.656                    24297285.348
        41.700          33.600
 123970578.525 6  96600687.91946  23590847.828                    23590851.262
        41.700          37.700
 113656163.213 7  88563316.41646  21628032.641                    21628035.969
        45.900          37.400
 117622923.601 7  91654218.51146  22382878.984                    22382878.813
        43.800          41.000
 127333609.505 6  99037179.686 6  23845468.188    23845467.883    23845468.355
        40.900          38.300
 126509430.909 7  98396229.586 5  23682832.180    23682831.078    23682833.363
```

**Figure 14 Data RINEX information**

## 4.3 Raw data to RINEX

Data obtained from receiver *.T0* needs to be convert to RINEX for that is necessary use RUNPKR (Trimble) and TEQC (Unavco); RUNPKR for convert raw data (*.T0*) to *.dat and TEQC for convert *.dat to RINEX.

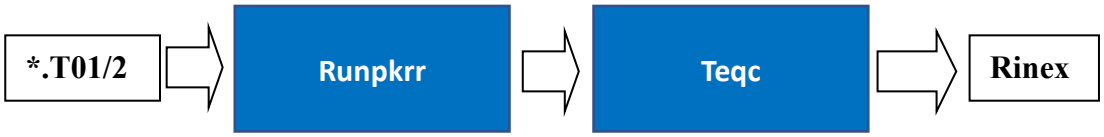


**Figure 15 Steps for convert raw data to RINEX**

## 4.4 Quality Check

Check the quality using the QC portion, which is a process for quality checking static

and kinematic dual-frequency GPS. The basic step is that linear combination (LC) of the pseudorange and carrier phase observations are used to compute L1 pseudorange multipath for C/A- or Pcode-observations, L2 pseudorange multipath for Pcode-observations, ionospheric phase effects, and the rate of change of the ionospheric delay. Information about the receiver clock slips, receiver cycle slips (receiver loss of tracking of L1 and/or L2), site multipath, satellite elevation and azimuth angles, receiver clock drift, receiver signal-noise ratios and other useful parameters and tracking statistics is written to a summary file. The QC report is called *.S which gives the main useful components related to the stations surroundings and data quality. MP1, MP2 and o/slps (complete observation/slips above 10 elevation) are always collected and studied. MP1 evaluates the pseudorange multipath and MP2 shows the pseudorange multipath and the noise intensity of the receivers. o/slps is always represented as CSR, which can be calculated with the formula 4.1:

$$CSR = \frac{1000}{o/slps} \tag{4.1}$$

RINEX observation files → teqc.exe → Quality check files (*. S)

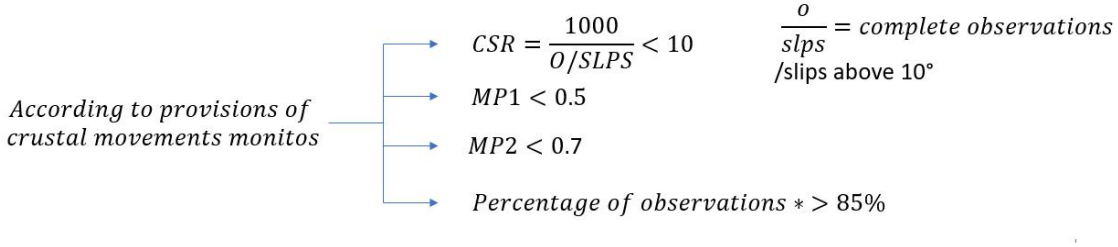


**Figure 16 Parameters for good quality data considerations**

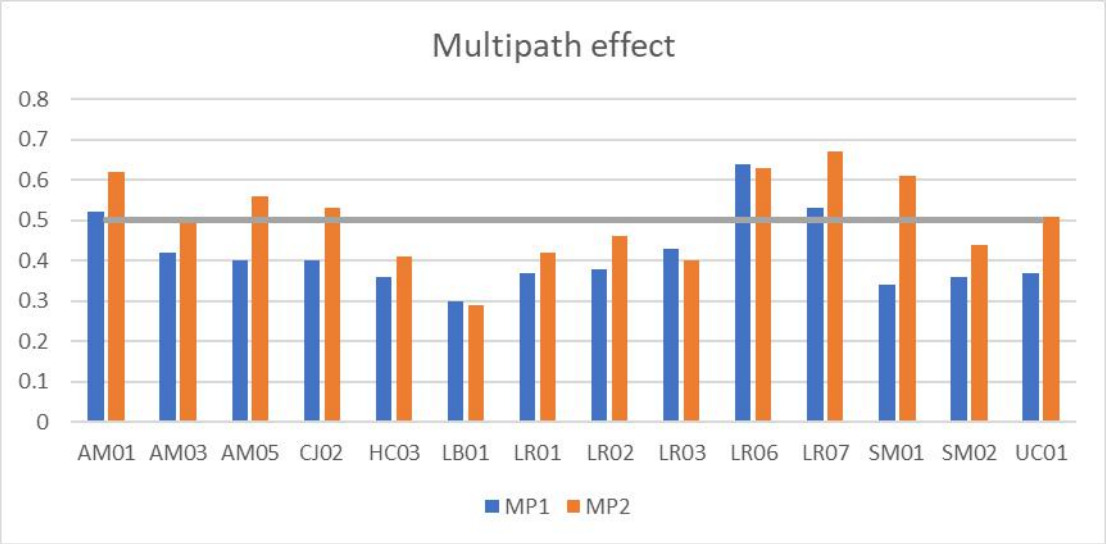


**Figure 17 Quality Check – Multipath validation**

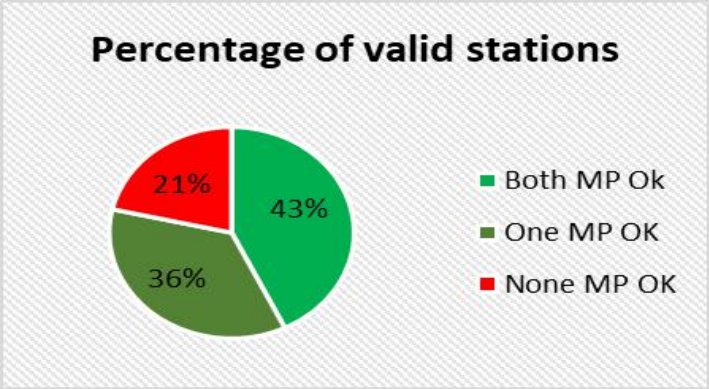


**Figure 18 Percentage of valid stations**

**Table 3 Data Quality Check, MP**

| Both MP OK | One MP OK | None MP OK |
|---|---|---|
| HC03 | AM03 | AM01 |
| LB01 | AM05 | LR06 |
| LR01 | CJ02 | LR07 |
| LR02 | SM01 | --- |
| LR03 | UC01 | --- |
| SM02 | --- | --- |

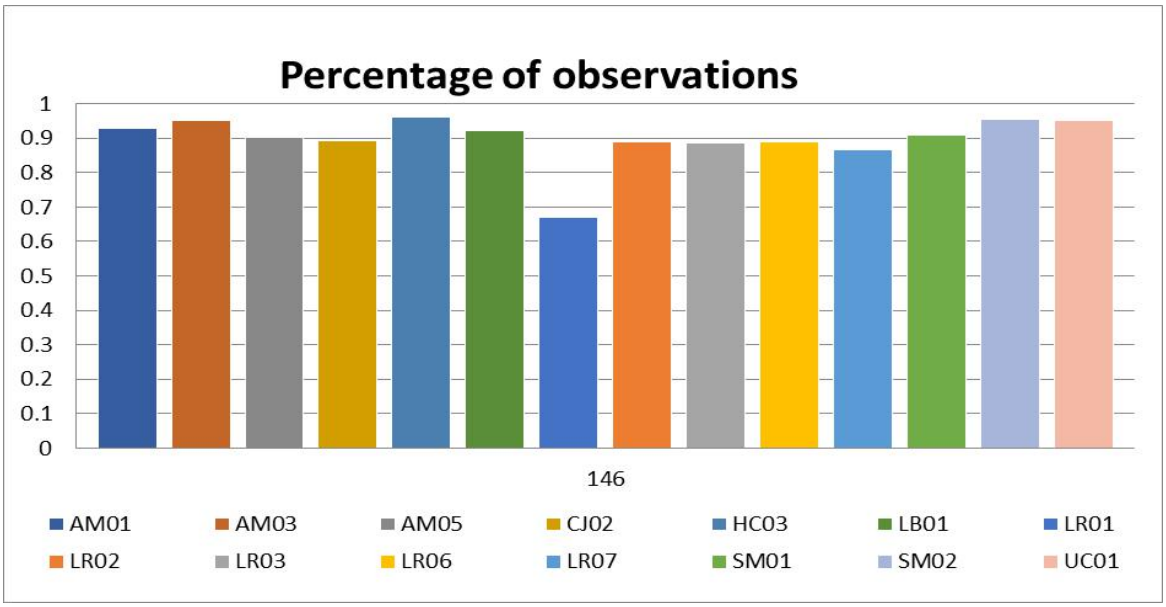


**Figure 19 Quality Check – Percentage of observations & CSR Validation**

Percentage of observation of station LR01 = 67.18% <85%. (BAD)

All stations satisfy CSR <10 criteria. (GOOD)

Validated stations after quality check

Observation Files

Data extracted from TEQC.exe SOFTWARE

Code for GNSS constellation:

Nothing → GPS

R → GLONASS

E →GALILEO

S →SBAS

B →BEIDOU

Symbology meaning:

o → Good observation data

L →rx lost clock

I → Ionospheric phase slip

- → No data SV above elev mask

M → Multipath slip

N → Good observation data

c → no data L1 C1 (only L2 C2)

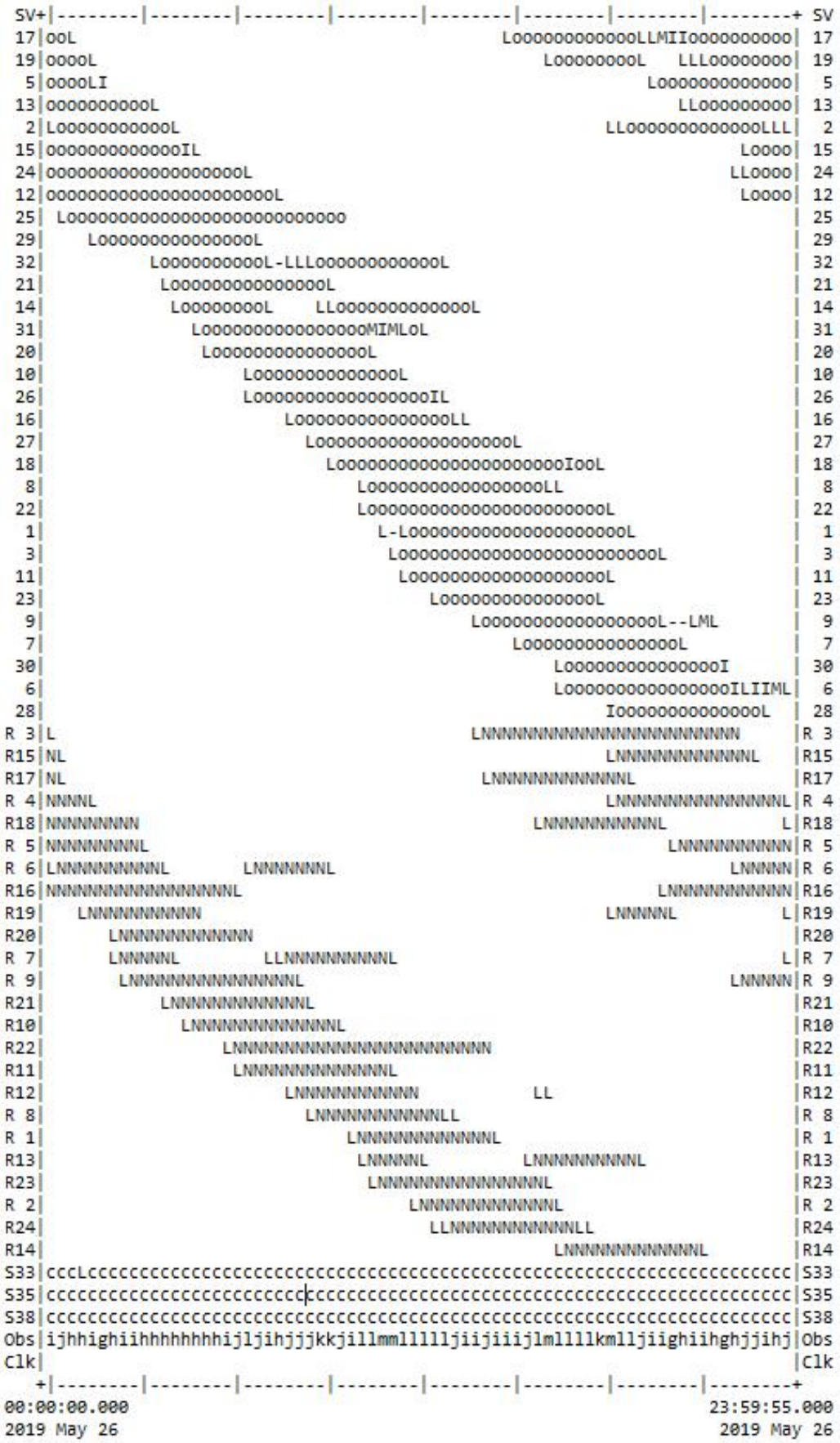

**Figure 20 Quality check information**

Observation Files

Data extracted from RTKLIB SOFTWARE

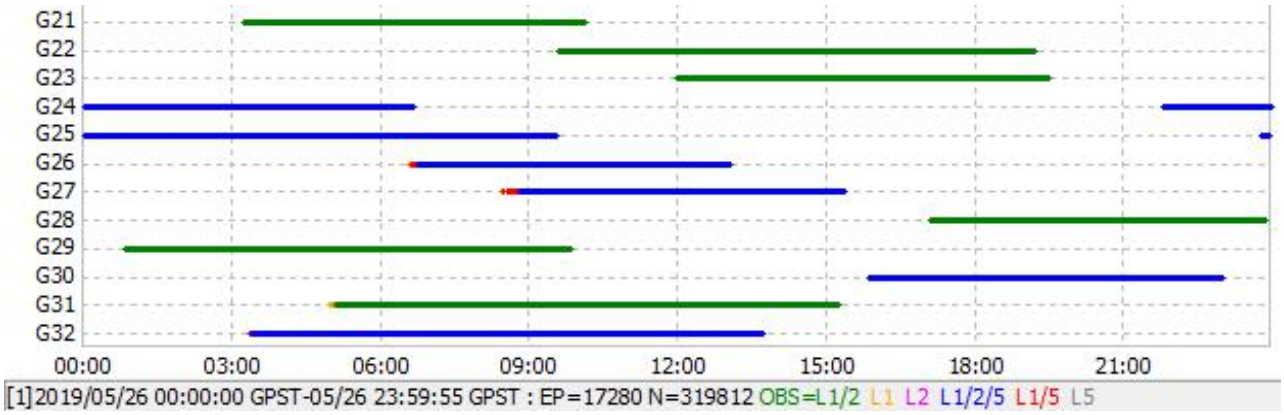


**Figure 21 Satellite visibility**

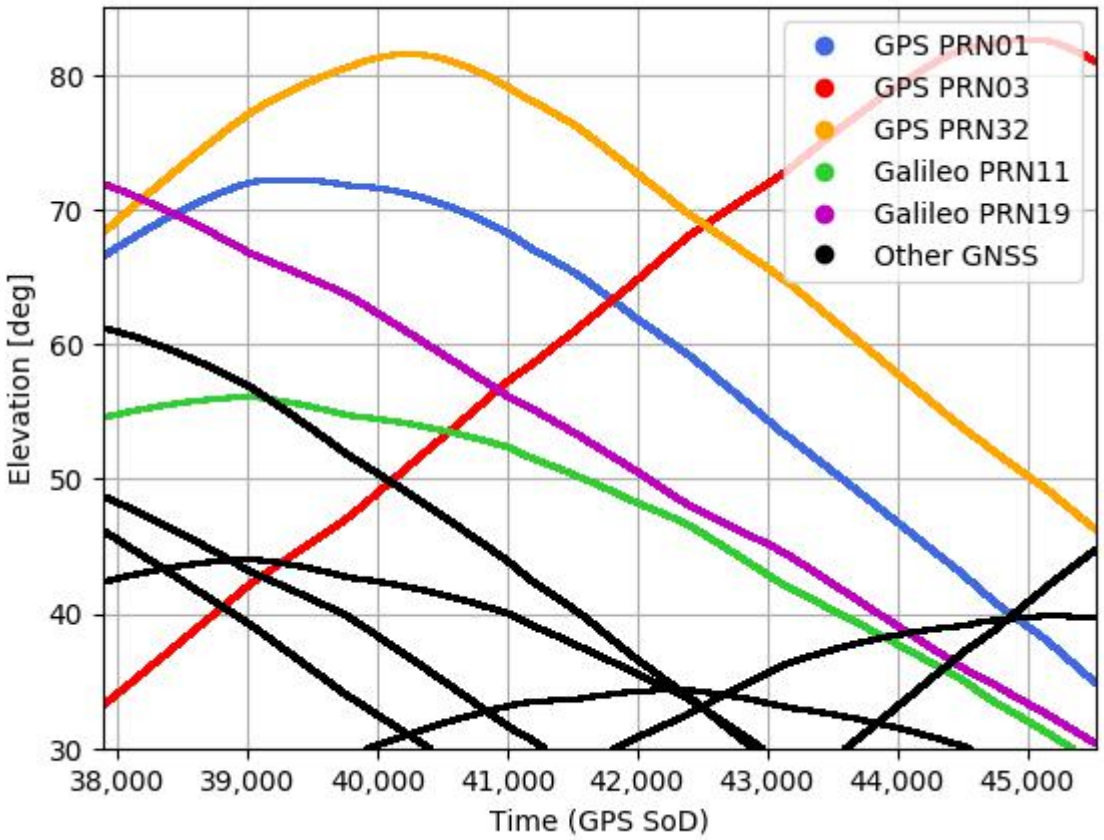


**Figure 22 Satellite elevation angle**

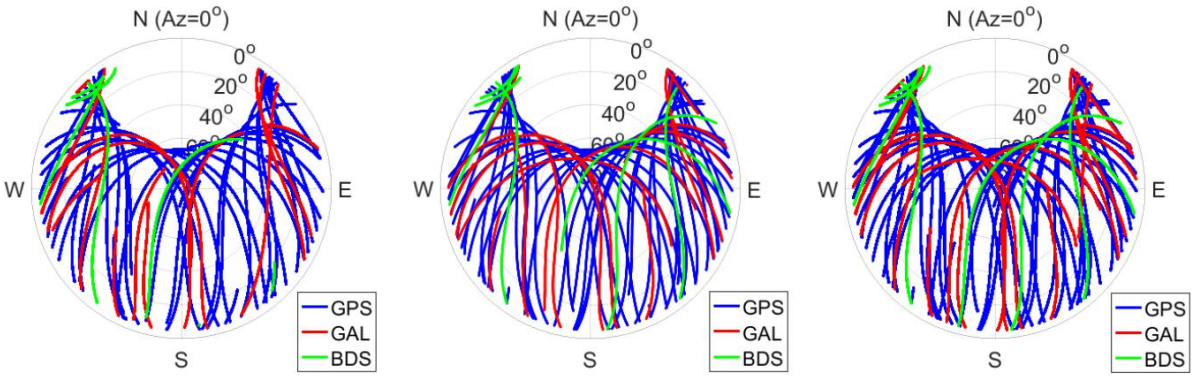


**Figure 23 Sky plot**

## 4.5 Data processing

### 4.5.1 Download metadata (Orbit and Clock)

For process data RINEX in PANDA we need download metadata, necessary for process this information.

The PPP technique is performed within the reference frame provided by the precise satellite orbit and precise clock products. The broadcast ephemeris has a typical accuracy about 1 meter for satellite position, which is not suitable for cm-level PPP data processing, but can be used for data preprocessing. In PANDA software, the broadcast ephemeris data is also needed for some purposes.

The final IGS GPS ephemeris and clock products are adopted for GPS PPP, which have an accuracy of 2.5 cm (1D mean RMS) for satellite position and 20ps (standard deviation) for satellite clock, respectively, as well as a typical latency about 12~18 days (http://www.igs.org/products).

The IGS precision orbit products are in the SP3 format. It follows the naming rule: igsWWWWD.sp3, where the WWWWD is the 5-character GPS week number the day of week (for example: May 5th, 2013 in GPS Time is 17390, which means the GPS week number is 1739, and the day of week is 0).

The IGS precision clock products follow the naming rule: igsWWWWD.clk. Particularly, igsWWWWD.clk often contains the clock errors in 300-second interval, which is very suitable for processing data at 300-second interval. But when we need to process the 30-second interval data, we need the 30-second interval clock products:

igsWWWWD.clk_30s. For even higher sample rate, we will need the codWWWWD.clk_05s products which is in 5-second interval.

It should be noted the IGS products are provided daily, which means it only contains the satellite position and clock error information during the particular day which is referred to its file name. (For example, igs17390.sp3 only contains the satellite orbits information on May 5th, 2013). So, we have to prepare the IGS products for the particular time of the observation data. But for the PANDA software, it often needs 3 days products for interpolation. For example:

If the RINEX data is on May 5th, 2013 (such as BJFS1250.13o), we will need the 3-consecutive-day products (the date of the observation is in the middle): igs17386.sp3 (17386 in GPS time is May 4th, 2013), igs17390.sp3 (17390 in GPS time is May 5th, 2013), igs17391.sp3, igs17386.clk, igs17390.clk, igs17391.clk.

The IGS products can be downloaded from the CDDIS ftp server:

- ✓ ftp://cddis.gsfc.nasa.gov/pub/gps/products/WWWW/igsWWWWD.sp3.Z
- ✓ ftp://cddis.gsfc.nasa.gov/pub/gps/products/WWWW/igsWWWWD.clk.Z

for example, the products on July 10th, 2013, the links for downloading the data is :

- ✓ ftp://cddis.gsfc.nasa.gov/pub/gps/products/1748/igs17483.sp3.Z
- ✓ ftp://cddis.gsfc.nasa.gov/pub/gps/products/1748/igs17483.clk_30s.Z

### 4.5.2 PANDA processing

The PANDA software includes many modules:

- ✓ Clnrnx: observation data preprocessing. This module will check the observation quality, detect the cycle slip and gross errors in the carrier phase observations. It will also cancel the arcs with too little available epochs. After running clnrnx, log files will be generated, which contains the arcs, ambiguities information.
- ✓ Mergesp3: this module will merge the 3- consecutive-day products (Sp3 and Clk products) to one single file.

- ✓ Sp3orb: this module will convert the merged sp3 file to a binary file, which contains the GPS orbits information. We do this for fast orbit interpolation.
- ✓ Lsq: this the Estimator which estimates the parameters including station position, receiver clock error, ZTDs, etc.
- ✓ Up_sit: this module will renew the a priori station coordinates.
- ✓ Extclk: this module will extract the receiver clock errors from the res- file which is generated from Lsq.
- ✓ Edtres: this module will check the observations again. Since more precise coordinates are estimated, the threshold for check data will be reduced down gradually.
- ✓ Mkztd: this module will extract the ZTD from the res- file which is generated from Lsq.

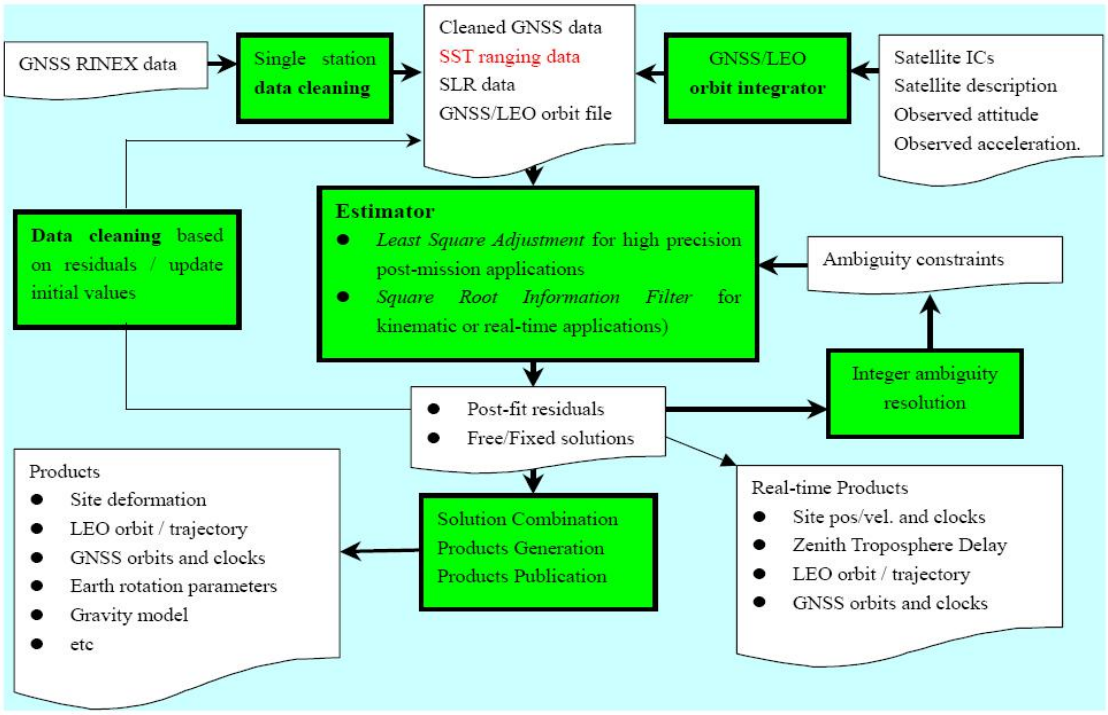


**Figure 24 Modules of PANDA for process**

### 4.5.3 Instruction on precise point positioning using PANDA

Dual frequency are code range and carrier phase are using in this PANDA software for PPP (Precise Point Positioning) technique. We know ionosphere delay is one main error in GNSS data observations. This dual frequency can enumeration this ionosphere delay. Other GNSS observation error is troposphere delay, multipath error, satellite clock error, receiver

clock error still. Dual frequency are code range and carrier phase called respectably PC and LC. GNSS data observation equation of Precise Point Positioning is given below:

$$Q^l(k) = \beta^l(k) + c(\partial t(k) - \partial T^l(k)) + ZTD(k).A(b^l(k)) + \theta_\omega \tag{4.2}$$

$$R^l(k).\mu = \beta^l(k) + c(\partial t(k) - \partial T^l(k)) + ZTD(k).A(b^l(k)) + D^l(k).\mu + \theta_\varphi \tag{4.3}$$

Where,

k = Epoch number

l = Satellite number

$Ql(k)$ = PC Observation

$Rl(k) = \ LC \ \ Observation$

$\beta l(k) = \ Distance \ \ between \ \ GNSS \ \ ground \ \ station \ \ and \ \ satellite$

$\partial t(k) = \ Receiver \ \ Error$

$\partial Tl(k) = \ Satellite \ \ clock \ \ error \ \ \mu = Wave \ \ length \ \ of \ \ ionosphere \ \ free$

$ZTD(k) = \ k-th \ \ epoch \ \ of \ \ Zenith \ \ Total \ \ Delay$

$A(bl(k)) \ \ = Mapping \ \ function \ \ of \ \ ZTD \ \ and$

$bl(k) = \ Satellite \ \ elevation \ \ engle$

$Dl(k) = \ ionosphere \ \ free \ \ ambiguity \ \ of \ \ l-th \ \ with \ \ satellite \ \ k-th \ \ epoch$

$\theta\omega \ = \ Multipath \ \ Error$

$\theta\varphi \ = \ Observation \ \ Error$

IGS provided all kinds of products for example in this PANDA software we get all satellite orbit and clock products get from IGS side. Phase center variation (PCV) and other important things antenna phase center offset (PCO). Those two-error correction from IGS. We know with weather conditions of ZTD component changes conspicuously. In Precise Point Positioning processing PPP system ZWD use the piece-wise constant (PWC) parameter for estimation.

### 4.5.4 Data preparation for precise point positioning

In this PANDA software for PPP RINEX Observation data, RINEX broadcast ephemeris and GPS satellite orbit and clock products is most three important parts. I get GNSS data since May 19 (139 JD) until June 2 (153 JD) of 2019, observation data from my country. This

observation data should be RINEX 2.11 format. And also, this data day by day 24 hours. Other most important data BRDC RINEX broadcast ephemeris and GPS satellite orbit and clock products collects from IGS side as same date like my country's observation file.

**Table 4 GNSS data collections information**

| Data Type | Date | Example | Download Source |
|---|---|---|---|
| Raw Data | 19/05/2019 – 02/06/2019 | SITEDOY0.T02 | Survey of Peru |
| Rinex Observation | 19/05/2019 – 02/06/2019 | SITEDOY0.YYo | Survey of Peru - TEQC |
| RINEX Broadcast ephemeris | 19/05/2019 – 02/06/2019 | brdcDOY0.YYn | IGS site or any web side – IGS Final |
| Satellite Orbit | 19/05/2019 – 02/06/2019 | igsWWWWD.sp3 | IGS site or any web side – IGS Final |
| Clock Products | 19/05/2019 – 02/06/2019 | igsWWWWD.clk_30s | IGS site or any web side – IGS Final |

### 4.5.5 GNSS station diagram

In this research used GNSS station high accuracy, these GNSS receiver are distributed a long territory of Peru, and these are located according international standards.


**Figure 25 Monument of GNSS station**

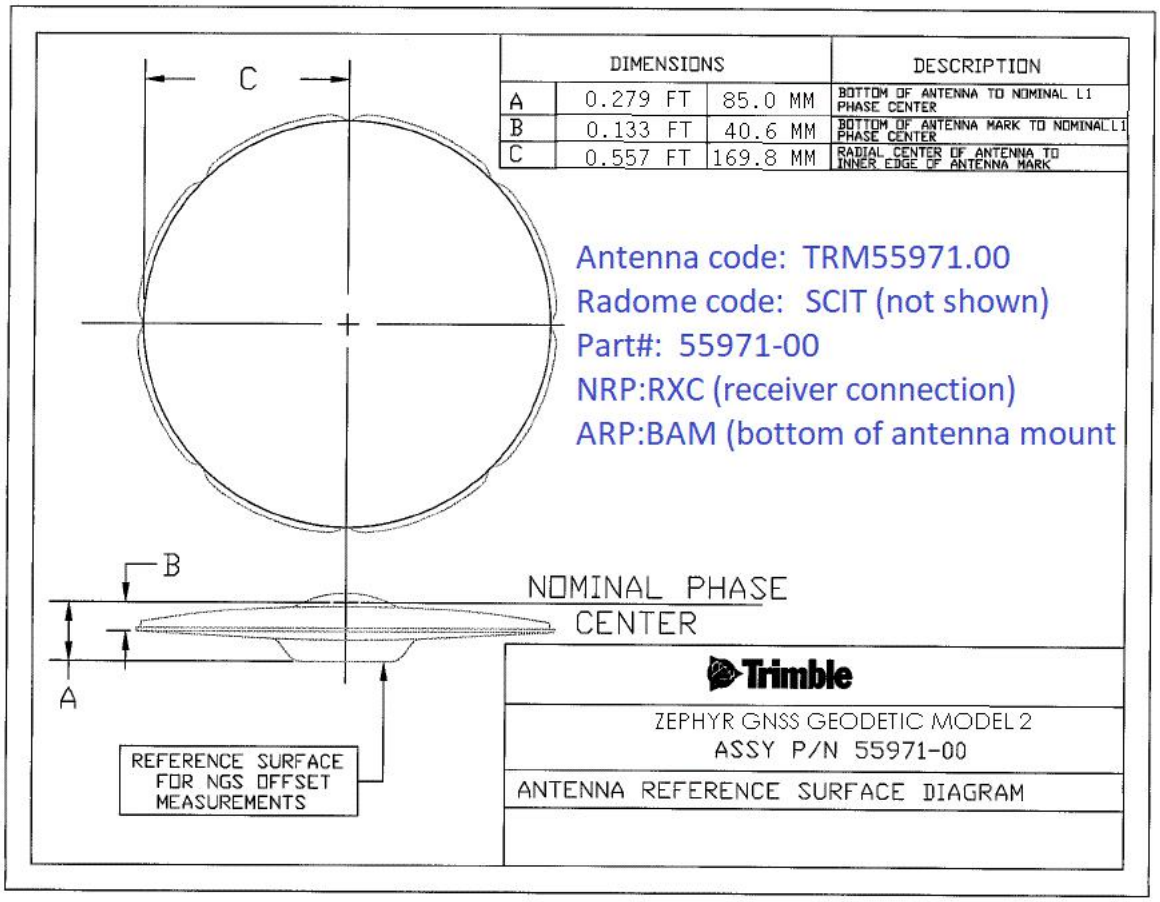


**Figure 26 Antenna diagram (www.trimble.com)**

# 5 Examples and Results

## 5.1 Research area and data

This research is focus on GNSS data processing of 14 GNSS stations surrounding earthquake 8 MW magnitude, analysis before and after earthquake, the main of this research is know the behavior and displacement occurred because earthquake. Data of whole GNSS stations was processed in PANDA software. In this thesis depends on two main tasks, first one is high accuracy GNSS RINEX data processing and other most important determination displacement occurred of earthquake and analysis part.

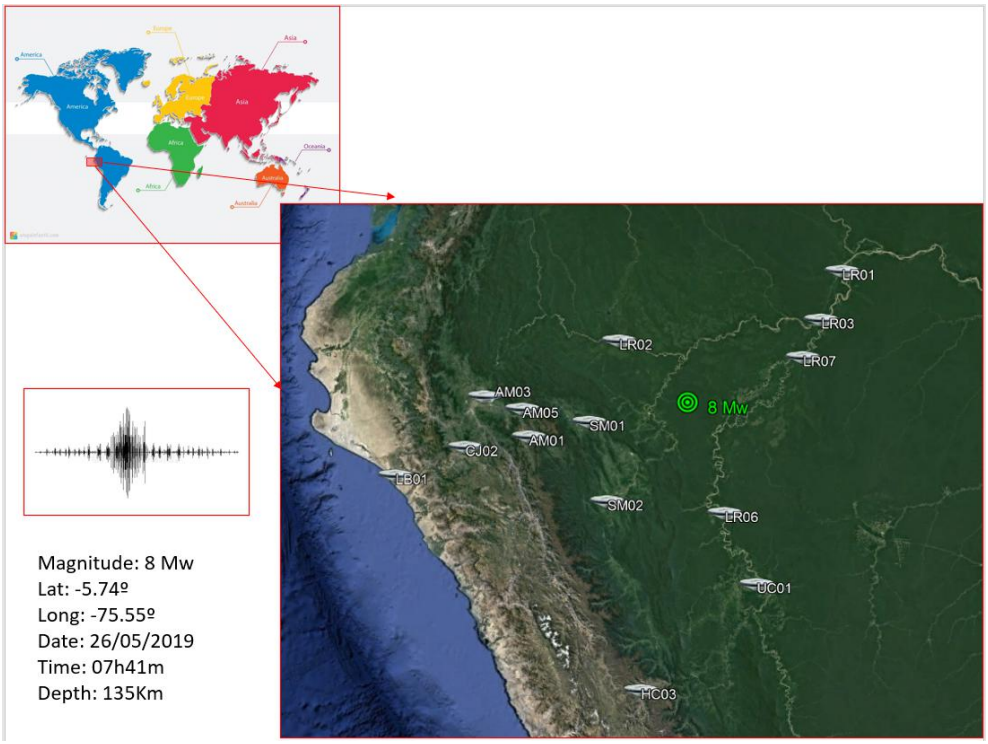


**Figure 27 Location GNSS stations sites**

The collects GPS raw data was extract from backup of National Geographic Institute of Peru (https://www.gob.pe/ign).

As we can see in the table 5, the distance between GNSS station and epicenter earthquake, the station more near is the LR02 station with 148 km, located in northwest part from epicenter, the LR07 and SM02 stations have little same distance but in opposite site, same to UC01, AM03 and LR01 with 320 km distance from epicenter, whole them different

directions respect to the epicenter, and finally the station more far is LB01, with 490 km from epicenter earthquake, this station is in the cost part of Peru exactly in the west part from epicenter.

These GNSS stations was selected to know the displacement each one and how is the behavior respect to the distance from epicenter and know the correlation with distance among them.

**Table 5 Distance between GNSS station and epicenter earthquake**

| / | Name | Distance (Km) |
|---|---|---|
| LR02 | San Lorenzo | 148 |
| SM01 | Moyobamba | 163 |
| LR06 | Contamana | 190 |
| LR07 | Requena | 202 |
| SM02 | Juanjui | 208 |
| LR03 | Nauta | 258 |
| AM01 | Chachapoyas | 263 |
| AM05 | Pomacochas | 270 |
| UC01 | Pucallpa | 316 |
| AM03 | Bagua | 328 |
| LR01 | Belen | 333 |
| CJ02 | Cutervo | 370 |
| HC03 | Huanuco | 474 |
| LB01 | Chiclayo | 490 |

**Table 6 GNSS station information**

| / | Name | Receiver | Antenna | Dome | Zone |
|---|---|---|---|---|---|
| LR02 | San Lorenzo | NET R9 TRIMBLE | Zephyr Geodetic model 3 | yes | 18 |
| SM01 | Moyobamba | NET R8 TRIMBLE | Zephyr Geodetic model 2 | yes | 18 |
| LR06 | Contamana | NET R9 TRIMBLE | Zephyr Geodetic model 3 | yes | 18 |
| LR07 | Requena | NET R9 TRIMBLE | Zephyr Geodetic model 3 | yes | 18 |
| SM02 | Juanjui | NET R8 TRIMBLE | Zephyr Geodetic model 2 | yes | 18 |
| LR03 | Nauta | NET R9 TRIMBLE | Zephyr Geodetic model 3 | yes | 18 |
| AM01 | Chachapoyas | NET R8 TRIMBLE | Zephyr Geodetic model 2 | yes | 18 |
| AM05 | Pomacochas | NET R9 TRIMBLE | Zephyr Geodetic model 3 | yes | 18 |
| UC01 | Pucallpa | NET R8 TRIMBLE | Zephyr Geodetic model 2 | yes | 18 |
| AM03 | Bagua | NET R8 TRIMBLE | Zephyr Geodetic model 2 | yes | 17 |
| LR01 | Belen | NET R8 TRIMBLE | Zephyr Geodetic model 2 | yes | 18 |
| CJ02 | Cutervo | NET R9 TRIMBLE | Zephyr Geodetic model 3 | yes | 17 |
| HC03 | Huanuco | NET R8 TRIMBLE | Zephyr Geodetic model 2 | yes | 18 |
| LB01 | Chiclayo | NET R8 TRIMBLE | Zephyr Geodetic model 2 | yes | 17 |

## 5.2 Data processing strategies for PPP

### 5.2.1 Error correction

Up to now we've been treating the calculations that go into GPS very abstractly, as if the whole thing were happening in a vacuum. But in the real world there are lots of things that can happen to a GPS signal that will make its life less than mathematically perfect.

These are errors induced by the satellite's location (Table 7). An 'ephemeris error'

describes the difference between the expected and actual orbital position of a GNSS satellite. Because GNSS receivers use the satellite's location in pseudorange calculations, orbital error reduces GNSS accuracy.

**Table 7 Error correction**

| Error | Correction |
|---|---|
| Error | Correction |
| Orbit | Sp3, IGS final precise ephemeris |
| Clock | Precise clock products, 30 seconds interval |
| Ionosphere | Ionosphere free linear combination |
| Troposphere | Calculate using Saastamoinen model and parameter estimation |
| PCO (Satellite phase center offset) | Correction of GPS |
| PCV (Satellite phase center variation) | Correction of GPS |
| Elevation angle cutoff | 5° |

### 5.2.2 Parameter

The most important result obtained from PANDA is the ac-curate estimate of the position of GNSS stations. Besides, PANDA also estimates the orbital and Earth-rotation parameters, zenith delays, and phase ambiguities by fitting to doubly differenced phase observations with the incorporation of a weighted least-squares algorithm. Since the functional (mathematical) model that relates observations to parameters is nonlinear, PANDA produces two solutions: the first provides coordinates within a few decimeters, and the second gives the final estimates.

This step requires the user to specify a priori finite constraint for each estimated parameter (Table 8). To avoid biasing the combination, PANDA generates the solution used by PANDA with loose parameter constraints. However, since phase ambiguities must be resolved (if possible) in phase processing, PANDA also generates several intermediate solutions with user-defined constraints before loosening the constraints for its final solution.

**Table 8 Parameter**

| Parameter name | Assessment |
|---|---|
| Coordinate | X, Y, Z site observation station coordinate, 5 second interval |
| Clock | Epoch-wise, 5 seconds |
| ZTD | 2-hours precise wise constant (PWC) |
| Ambiguity | Estimated as constant, the ambiguities between a baseline-by-baseline it resolved |

## 5.3 GNSS stations coordinates displacement result analysis

### 5.3.1 AM01 station

Distance between earthquake epicenter to AM01 station is 263 Km, and the result about data processing is show in Figure 28, as we can see mild displacement in North and East. In the component North we can see mild displacement to south and, in the component, mild displacement to west, and in the component Up not much variability, only some stuttering reason is why in vertical component always we cannot get good accuracy after processing.

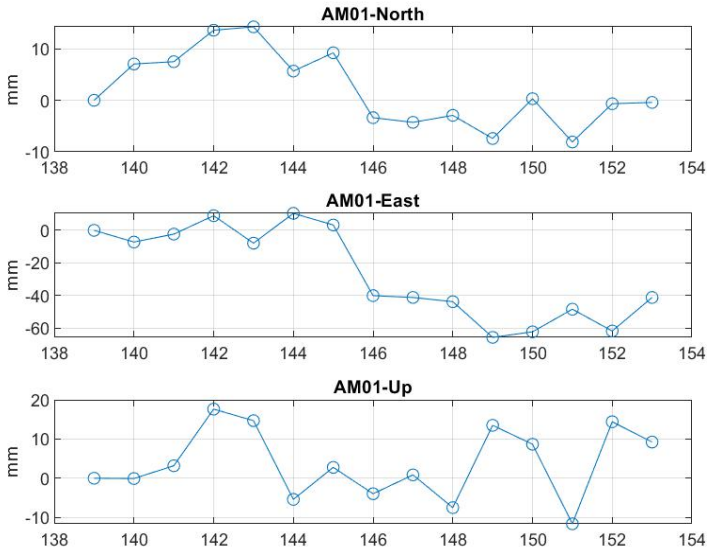


**Figure 28 AM01 station daily North, East and Up direction position**

As we can see in the table 9, we can see the ENU coordinates, considering the first day

in zero as the initial coordinate, we can see the next day's how is changing along the days before and after earthquake, in the red 146 doy represent earthquake, after that occurred a displacement 5.27 cm west and 1.15 cm south direction.

**Table 9 AM01 station daily coordinate towards the east north and up direction (cm)**

| Doy | E | N | U |
|---|---|---|---|
| 139 | 0.00 | 0.00 | 0.00 |
| 140 | -0.72 | 0.71 | -0.01 |
| 141 | -0.23 | 0.75 | 0.32 |
| 142 | 0.90 | 1.36 | 1.76 |
| 143 | -0.79 | 1.43 | 1.47 |
| 144 | 1.04 | 0.57 | -0.54 |
| 145 | 0.33 | 0.92 | 0.28 |
| 146 | -4.00 | -0.34 | -0.40 |
| 147 | -4.11 | -0.43 | 0.09 |
| 148 | -4.37 | -0.29 | -0.75 |
| 149 | -6.55 | -0.74 | 1.35 |
| 150 | -6.21 | 0.03 | 0.87 |
| 151 | -4.83 | -0.81 | -1.16 |
| 152 | -6.16 | -0.07 | 1.44 |
| | **Average E** | **Average N** | **Average U** |
| **BE:** | 0.08 | 0.82 | 0.47 |
| **AE:** | -5.19 | -0.34 | 0.39 |
| **Δ:** | -5.27 | -1.15 | -0.08 |

### 5.3.2 AM03 station

The AM03 station is located in Amazonas city, and the distance between earthquake epicenter to AM03 station is 328 Km, and the result about data processing is show in Figure 29, as we cannot see much displacement. In the component North and west they can see the average is constant, little catering surrounding 1cm we can say not much displacement the this GNSS station, and in the component Up not much variability, only some stuttering reason is why in vertical component always we cannot get good accuracy after processing.

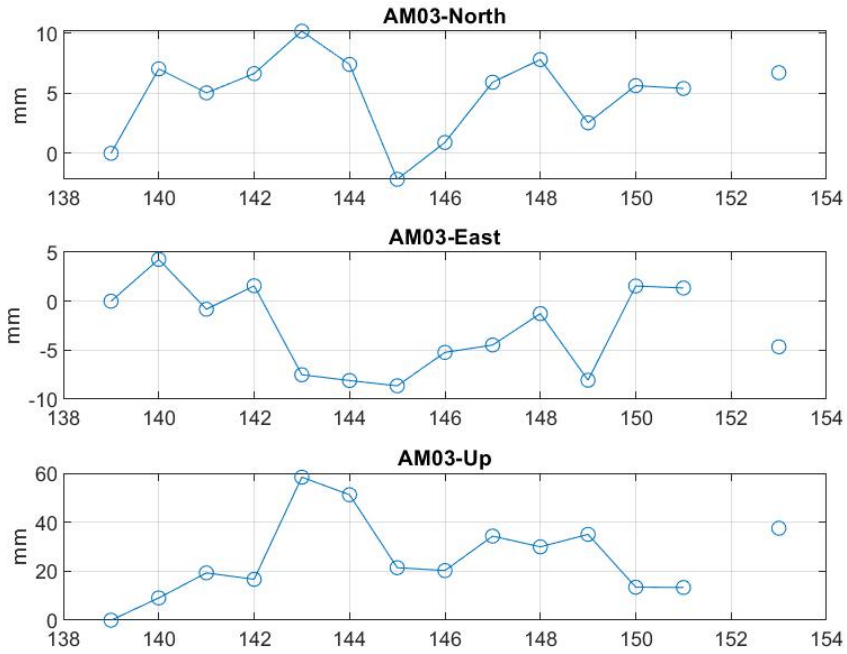


**Figure 29 AM03 station daily North, East and Up direction position**

As we can see in the table 10, we can see the ENU coordinates, considering the first day in zero as the initial coordinate, we can see the next day's how is changing along the days before and after earthquake, in the red 146 doy represent earthquake, after that occurred a displacement 0.02 cm east and 0.08 cm north direction, actually We cannot see enough displacement in this GNSS station.

**Table 10 AM03 station daily coordinate towards the east north and up direction (cm)**

| Doy | E | N | U |
|---|---|---|---|
| 139 | 0.00 | 0.00 | 0.00 |
| 140 | 0.43 | 0.70 | 0.91 |
| 141 | -0.08 | 0.50 | 1.93 |
| 142 | 0.16 | 0.66 | 1.67 |
| 143 | -0.75 | 1.02 | 5.84 |
| 144 | -0.81 | 0.74 | 5.12 |
| 145 | -0.86 | -0.22 | 2.14 |
| 146 | -0.52 | 0.09 | 2.03 |
| 147 | -0.45 | 0.59 | 3.43 |
| 148 | -0.13 | 0.78 | 2.99 |
| 149 | -0.81 | 0.25 | 3.51 |
| 150 | 0.16 | 0.56 | 1.35 |
| 151 | 0.13 | 0.54 | 1.34 |
| 152 | NaN | NaN | NaN |
| 153 | -0.47 | 0.67 | 3.76 |
| | **Average E** | **Average N** | **Average U** |
| **BE:** | -0.27 | 0.49 | 2.52 |
| **AE:** | -0.26 | 0.57 | 2.73 |
| **Δ:** | 0.02 | 0.08 | 0.21 |

Also, we can see the average coordinate before earthquake surrounding -0.27 cm in component west and 0.49 in component north, after earthquake changed such as -0.26 cm east and 0.57 cm north, the result is a displacement south - east direction. In the case of vertical component, we cannot see displacements, only the movement was surrounding 0.8 mm, is a

little difference.

### 5.3.3 AM05 station

AM05 station is 270 Km from epicenter earthquake, and this station is little same to AM01 in radial distance from earthquake, in the figure 30 we can see the movement a long the time respect to earthquake, in North component we can see little change along the time, and in the East component significative change after earthquake, in the horizontal component the variability are surrounding 4 cm into 14 days processed.

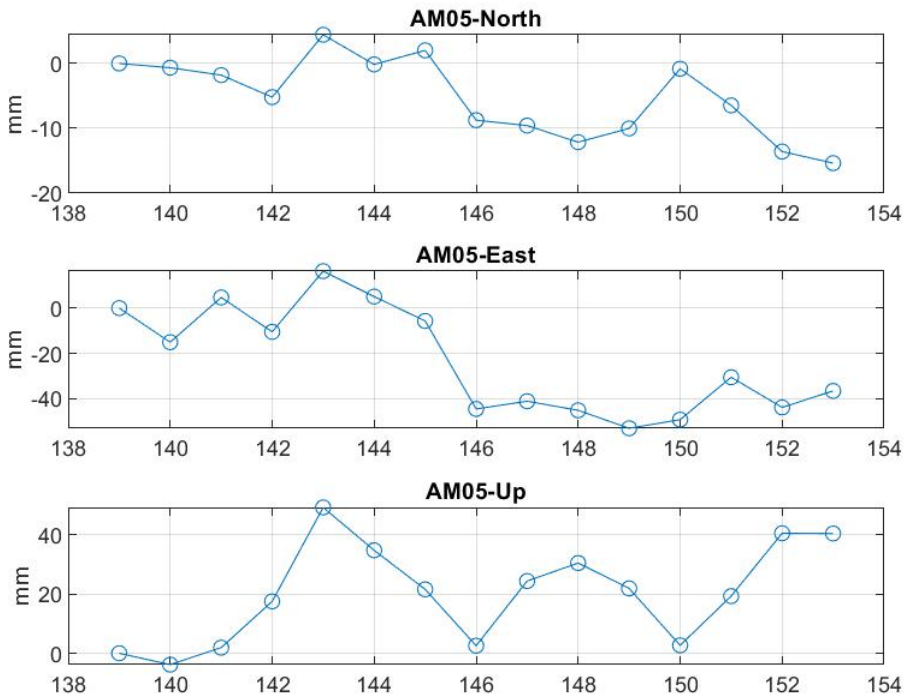


**Figure 30 AM05 station daily North, East and Up direction position**

In the table 11, We can see the coordinate day per day, processed in static mode, the red 146 doy represent the earthquake day, after that they change some centimeters as we can see in the figure 30 and table in mention. The coordinate is in ENU considering the first day as zero, the average coordinate before earthquake was -0.07 cm east and -0.02 north, after earthquake changed to -4.28 east and -0.97 north, in vertical component not much difference such as we can see in the table in mention.

**Table 11 AM05 station daily coordinate towards the east north and up direction (cm)**

| Doy | E | N | U |
|---|---|---|---|
| 139 | 0.00 | 0.00 | 0.00 |
| 140 | -1.50 | -0.07 | -0.38 |
| 141 | 0.47 | -0.18 | 0.19 |
| 142 | -1.05 | -0.52 | 1.75 |
| 143 | 1.63 | 0.44 | 4.93 |
| 144 | 0.51 | -0.01 | 3.48 |
| 145 | -0.57 | 0.20 | 2.16 |
| 146 | -4.45 | -0.87 | 0.26 |
| 147 | -4.11 | -0.96 | 2.44 |
| 148 | -4.51 | -1.21 | 3.05 |
| 149 | -5.30 | -1.00 | 2.19 |
| 150 | -4.92 | -0.08 | 0.27 |
| 151 | -3.05 | -0.65 | 1.93 |
| 152 | -4.38 | -1.36 | 4.05 |
| 153 | -3.65 | -1.54 | 4.05 |
| | **Average E** | **Average N** | **Average U** |
| **BE:** | -0.07 | -0.02 | 1.73 |
| **AE:** | -4.28 | -0.97 | 2.57 |
| **Δ:** | -4.20 | -0.95 | 0.84 |

Also, we can see the displacement occurred after earthquake, had 4.2 cm displacement west component and 0.95 cm to the south, surrounding 1 cm in this last component, in vertical component 0.84 cm up.

### 5.3.4 CJ02 station

Distance between earthquake epicenter to CJ02 station is 370 Km, and the result about data processing is show in Figure 31, as we can see mild displacement in North and East. In the component North we can see mild displacement to south and, in the component, mild displacement to west, and in the component Up not much variability, only some stuttering reason is why in vertical component always we cannot get good accuracy after processing.

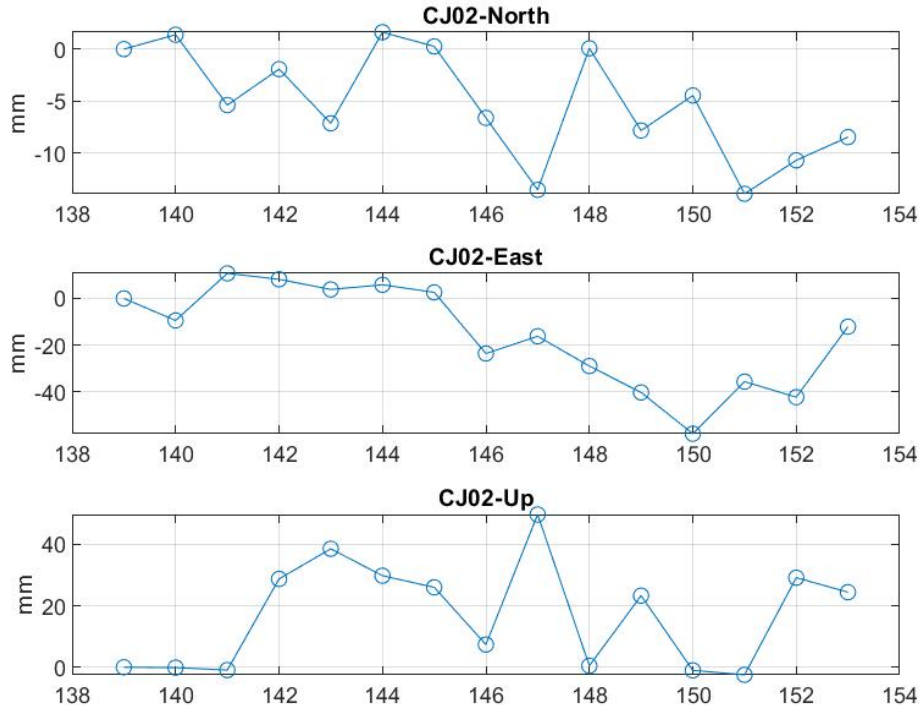


**Figure 31 CJ02 station daily North, East and Up direction position**

As we can see in the table 12, we can see the ENU coordinates, considering the first day in zero as the initial coordinate, we can see the next day's how is changing along the days before and after earthquake, in the red 146 doy represent earthquake, after that occurred a displacement 3.64 cm west and 0.68 cm south direction.

**Table 12 CJ02 station daily coordinate towards the east north and up direction (cm)**

| Doy | E | N | U |
|---|---|---|---|
| 139 | 0.00 | 0.00 | 0.00 |
| 140 | -0.94 | 0.14 | -0.01 |
| 141 | 1.07 | -0.54 | -0.09 |
| 142 | 0.82 | -0.19 | 2.87 |
| 143 | 0.38 | -0.71 | 3.85 |
| 144 | 0.58 | 0.16 | 2.98 |
| 145 | 0.26 | 0.03 | 2.60 |
| 146 | -2.35 | -0.66 | 0.74 |
| 147 | -1.62 | -1.35 | 4.97 |
| 148 | -2.89 | 0.01 | 0.05 |
| 149 | -4.02 | -0.78 | 2.33 |
| 150 | -5.78 | -0.45 | -0.10 |
| 151 | -3.56 | -1.39 | -0.25 |
| 152 | -4.22 | -1.07 | 2.91 |
| 153 | -1.21 | -0.85 | 2.44 |
| | **Average E** | **Average N** | **Average U** |
| **BE:** | 0.31 | -0.16 | 1.74 |
| **AE:** | -3.33 | -0.84 | 1.76 |
| **Δ:** | -3.64 | -0.68 | 0.02 |

Also, we can see the average coordinate before earthquake surrounding 0.31 cm in component east and 0.16 in component south, after earthquake changed such as 3.33 cm west and 0.84 cm south, the result is a displacement south - west direction. In the case of vertical component, we cannot see displacements, only the movement was surrounding 0.02 mm, is a

little difference.

### 5.3.5 HC03 station

HC03 station is 474 Km from epicenter earthquake, and this station is little same to LB01 in radial distance from earthquake, in the figure 32 we can see the movement along the time respect to earthquake, in North component we can see little change along the time, and in the East component significative change after earthquake, in the horizontal component the variability is surrounding 4 cm into 14 days processed.

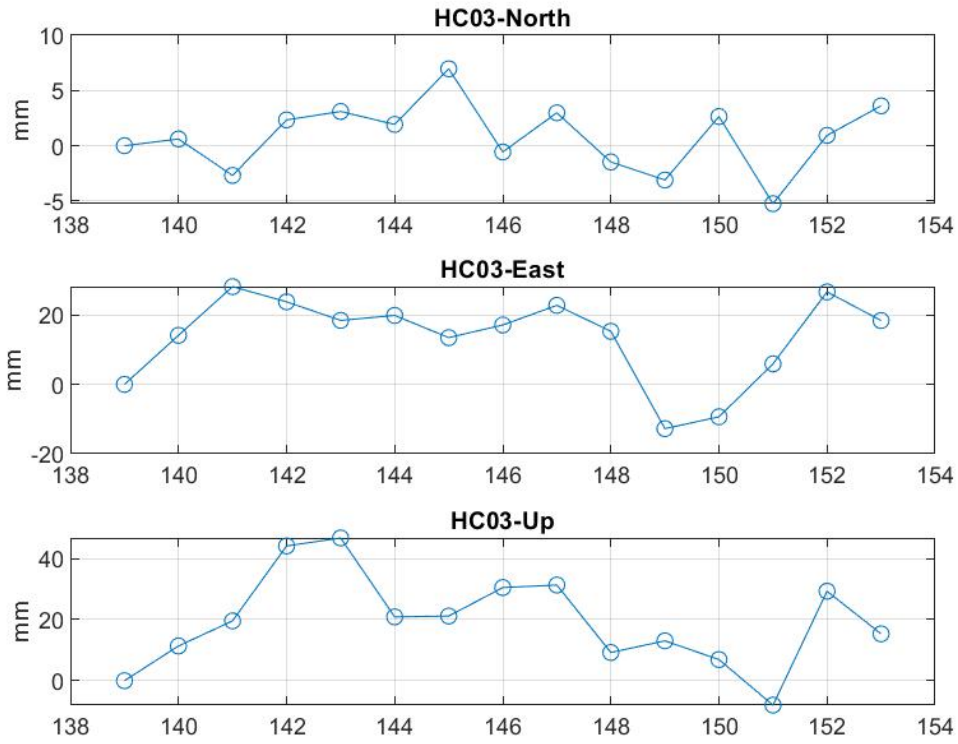


**Figure 32 HC03 station daily North, East and Up direction position**

In the table 13, we can see the coordinate day per day, processed in static mode, the red 146 doy represent the earthquake day, after that they change some centimeters as we can see in the figure 30 and table in mention. The coordinate is in ENU considering the first day as zero, the average coordinate before earthquake was 1.68 cm east and 0.16 north, after earthquake changed to 0.96 west and 0.17 south, in vertical component not much difference such as we can see in the table in mention.

**Table 13 HC03 station daily coordinate towards the east north and up direction (cm)**

| Doy | E | N | U |
|---|---|---|---|
| 139 | 0.00 | 0.00 | 0.00 |
| 140 | 1.41 | 0.06 | 1.14 |
| 141 | 2.82 | -0.27 | 1.96 |
| 142 | 2.38 | 0.23 | 4.41 |
| 143 | 1.84 | 0.31 | 4.67 |
| 144 | 1.99 | 0.19 | 2.09 |
| 145 | 1.35 | 0.70 | 2.12 |
| 146 | 1.71 | -0.06 | 3.05 |
| 147 | 2.28 | 0.30 | 3.13 |
| 148 | 1.53 | -0.15 | 0.92 |
| 149 | -1.28 | -0.31 | 1.30 |
| 150 | -0.93 | 0.26 | 0.69 |
| 151 | 0.59 | -0.52 | -0.80 |
| 152 | 2.66 | 0.09 | 2.93 |
| 153 | 1.84 | 0.36 | 1.53 |
| | **Average E** | **Average N** | **Average U** |
| **BE:** | 1.68 | 0.17 | 2.34 |
| **AE:** | 0.96 | 0.01 | 1.39 |
| **Δ:** | -0.73 | -0.17 | -0.95 |

Also, we can see the displacement occurred after earthquake, had 0.73 cm displacement west component and 0.17 cm to the south, surrounding 1 cm in this last component, in vertical component 0.95 cm down.

### 5.3.6 LB01 station

Distance between earthquake epicenter to LB01 station is 490 Km, and the result about data processing is show in Figure 33, as we can see mild displacement in North and East. In the component North we can see mild displacement to south and, in the component, mild displacement to west, and in the component Up not much variability, only some stuttering reason is why in vertical component always we cannot get good accuracy after processing.

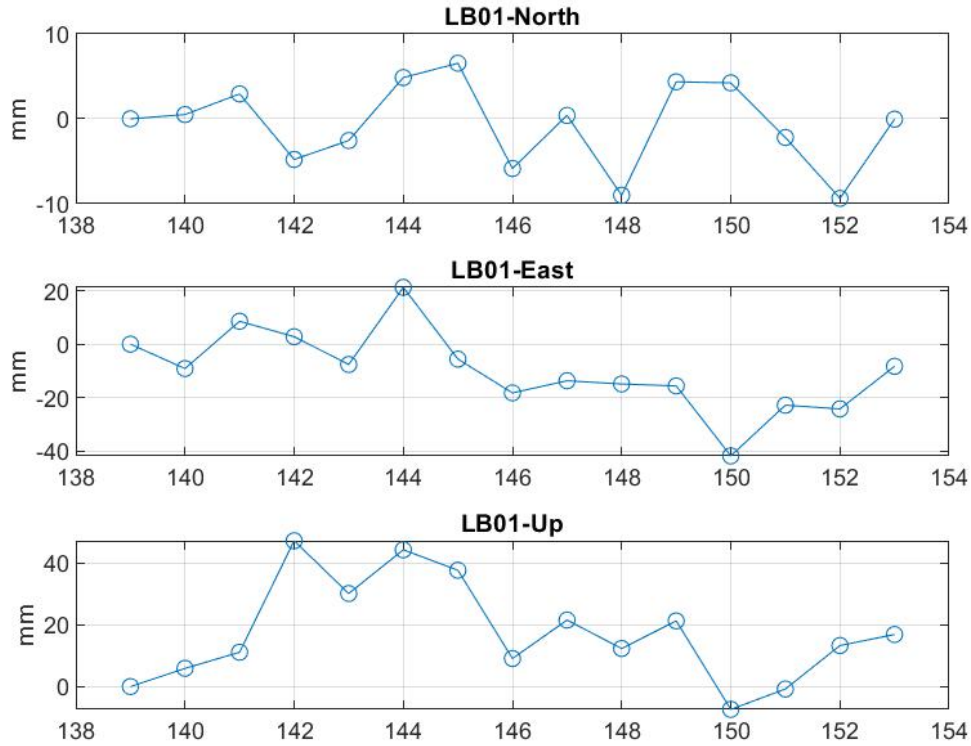


**Figure 33 LB01 station daily North, East and Up direction position**

As we can see in the table 14, we can see the ENU coordinates, considering the first day in zero as the initial coordinate, we can see the next day's how is changing along the days before and after earthquake, in the red 146 doy represent earthquake, after that occurred a displacement 2.17 cm west and 0.27 cm south direction.

**Table 14 LB01 station daily coordinate towards the east north and up direction (cm)**

| Doy | E | N | U |
|---|---|---|---|
| 139 | 0.00 | 0.00 | 0.00 |
| 140 | -0.91 | 0.05 | 0.59 |
| 141 | 0.86 | 0.29 | 1.11 |
| 142 | 0.28 | -0.48 | 4.72 |
| 143 | -0.76 | -0.26 | 3.02 |
| 144 | 2.12 | 0.49 | 4.43 |
| 145 | -0.56 | 0.65 | 3.77 |
| 146 | -1.82 | -0.59 | 0.91 |
| 147 | -1.37 | 0.04 | 2.15 |
| 148 | -1.49 | -0.90 | 1.23 |
| 149 | -1.56 | 0.44 | 2.13 |
| 150 | -4.18 | 0.42 | -0.74 |
| 151 | -2.28 | -0.22 | -0.08 |
| 152 | -2.42 | -0.94 | 1.33 |
| 153 | -0.83 | 0.00 | 1.69 |
| | **Average E** | **Average N** | **Average U** |
| **BE:** | 0.15 | 0.11 | 2.52 |
| **AE:** | -2.02 | -0.17 | 1.10 |
| **Δ:** | -2.17 | -0.27 | -1.42 |

Also, we can see the average coordinate before earthquake surrounding 0.15 cm in component east and 0.11 in component north, after earthquake changed such as 2.02 cm west and 0.17 cm south, the result is a displacement south - west direction. In the case of vertical component, we can see displacements, the displacement was 1.42 cm down.

### 5.3.7 LR01 station

LR01 station is 333 Km from epicenter earthquake, and this station is little same to AM03 and UC01 in radial distance from earthquake, in the figure 34 we can see the movement along the time respect to earthquake, in North component we can see little change along the time, and in the East component significative change after earthquake, in the horizontal component the variability is surrounding 4 cm into 14 days processed.

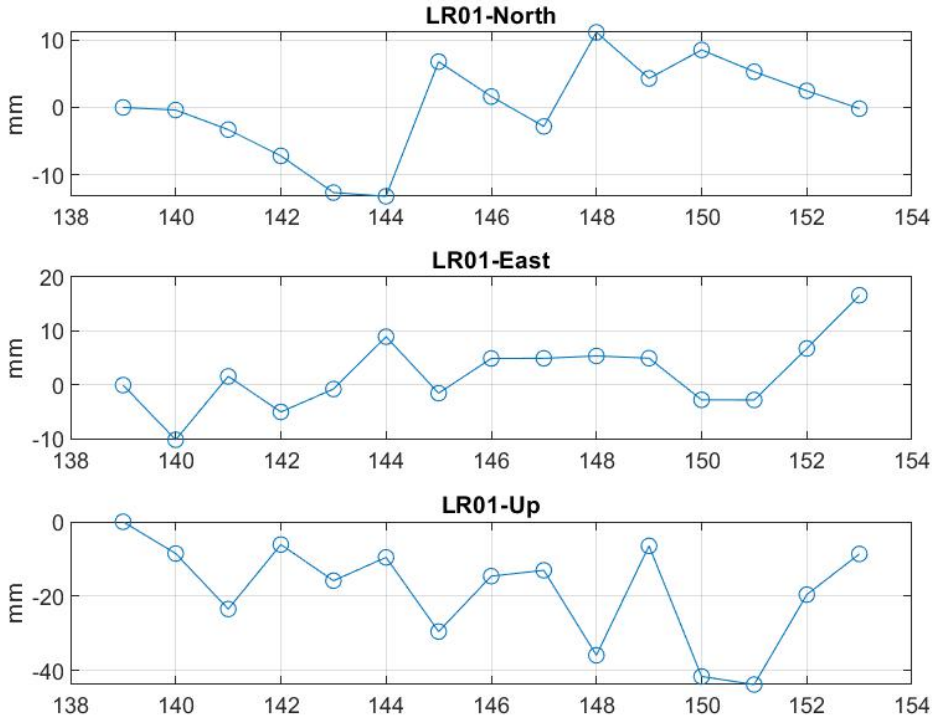


**Figure 34 LR01 station daily North, East and Up direction position**

In the table 15, we can see the coordinate day per day, processed in static mode, the red 146 doy represent the earthquake day, after that they change some centimeters as we can see in the figure 34 and table in mention. The coordinate is in ENU considering the first day as zero, the average coordinate before earthquake was 0.10 cm west and 0.43 south, after earthquake changed to 0.48 east and 0.41 north, in vertical component not much difference such as we can see in the table in mention.

**Table 15 LR01 station daily coordinate towards the east north and up direction (cm)**

| Doy | E | N | U |
|---|---|---|---|
| 139 | 0.00 | 0.00 | 0.00 |
| 140 | -1.01 | -0.04 | -0.85 |
| 141 | 0.16 | -0.33 | -2.35 |
| 142 | -0.50 | -0.72 | -0.61 |
| 143 | -0.07 | -1.26 | -1.58 |
| 144 | 0.90 | -1.32 | -0.96 |
| 145 | -0.15 | 0.68 | -2.95 |
| 146 | 0.49 | 0.16 | -1.46 |
| 147 | 0.50 | -0.28 | -1.30 |
| 148 | 0.54 | 1.11 | -3.59 |
| 149 | 0.50 | 0.43 | -0.65 |
| 150 | -0.27 | 0.85 | -4.16 |
| 151 | -0.28 | 0.53 | -4.38 |
| 152 | 0.68 | 0.25 | -1.96 |
| 153 | 1.66 | -0.02 | -0.86 |
| | **Average E** | **Average N** | **Average U** |
| **BE:** | -0.10 | -0.43 | -1.33 |
| **AE:** | 0.48 | 0.41 | -2.41 |
| **Δ:** | 0.57 | 0.84 | -1.09 |

Also, we can see the displacement occurred after earthquake, had 0.1 cm displacement west component and 0.43 cm to the south, surrounding 0.8 cm in this last component, in vertical component 1.09 cm down.

### 5.3.8 LR02 station

LR02 station is 148 Km from epicenter earthquake, and this station is little same to SM01 in radial distance from earthquake, in the figure 35 we can see the movement along the time respect to earthquake, in North component we can see little change along the time, and in the East component significative change after earthquake, in the horizontal component the variability is surrounding 5 cm into 14 days processed.

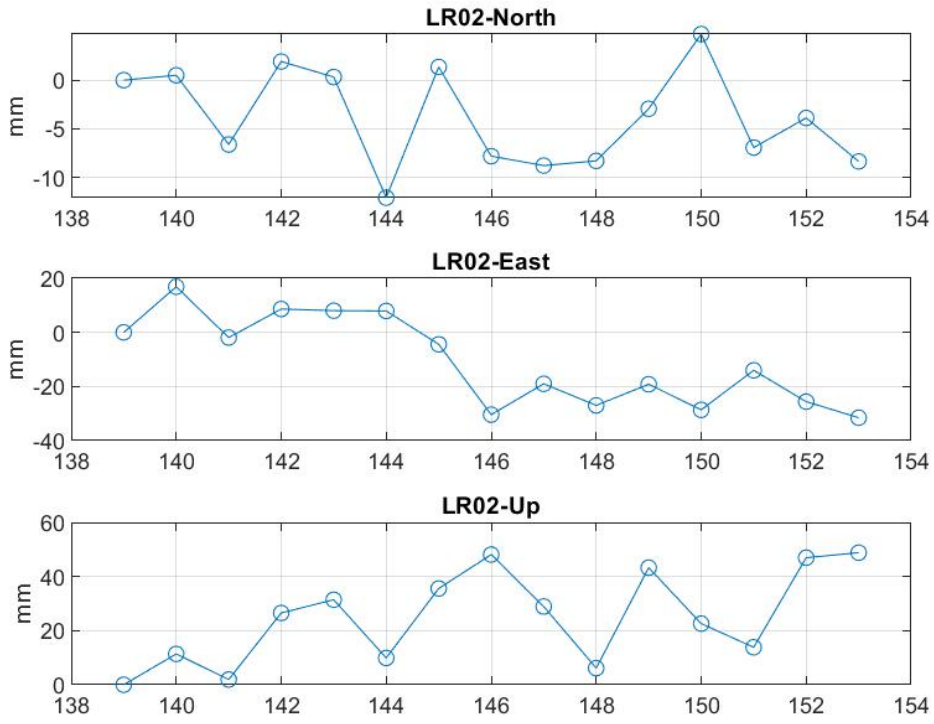


**Figure 35 LR02 station daily North, East and Up direction position**

In the table 16, we can see the coordinate day per day, processed in static mode, the red 146 doy represent the earthquake day, after that they change some centimeters as we can see in the figure 35 and table in mention. The coordinate is in ENU considering the first day as zero, the average coordinate before earthquake was 0.50 cm west and 0.21 south, after earthquake changed to 2.36 west and 0.49 south, in vertical component we can see a little increasing the from down to up.

**Table 16 LR02 station daily coordinate towards the east north and up direction (cm)**

| Doy | E | N | U |
|---|---|---|---|
| 139 | 0.00 | 0.00 | 0.00 |
| 140 | 1.69 | 0.05 | 1.14 |
| 141 | -0.19 | -0.66 | 0.19 |
| 142 | 0.86 | 0.19 | 2.65 |
| 143 | 0.80 | 0.03 | 3.14 |
| 144 | 0.79 | -1.21 | 0.99 |
| 145 | -0.44 | 0.14 | 3.56 |
| 146 | -3.04 | -0.78 | 4.81 |
| 147 | -1.90 | -0.88 | 2.89 |
| 148 | -2.70 | -0.83 | 0.62 |
| 149 | -1.92 | -0.29 | 4.33 |
| 150 | -2.86 | 0.47 | 2.26 |
| 151 | -1.40 | -0.69 | 1.38 |
| 152 | -2.56 | -0.39 | 4.70 |
| 153 | -3.15 | -0.83 | 4.88 |
| | **Average E** | **Average N** | **Average U** |
| **BE:** | 0.50 | -0.21 | 1.67 |
| **AE:** | -2.36 | -0.49 | 3.01 |
| **Δ:** | -2.86 | -0.28 | 1.34 |

Also, we can see the displacement occurred after earthquake, had 2.86 cm displacement west component and 0.28 cm to the south, surrounding 2 cm in this last component, in vertical component 1.34 cm up.

### 5.3.9 LR03 station

LR03 station is 258 Km from epicenter earthquake, and this station is little same to AM01 and AM05 in radial distance from earthquake, in the figure 36 we can see the movement along the time respect to earthquake, in North component we can see little change along the time, and in the East component significative change after earthquake, in the horizontal component the variability is surrounding 6 cm into 14 days processed.

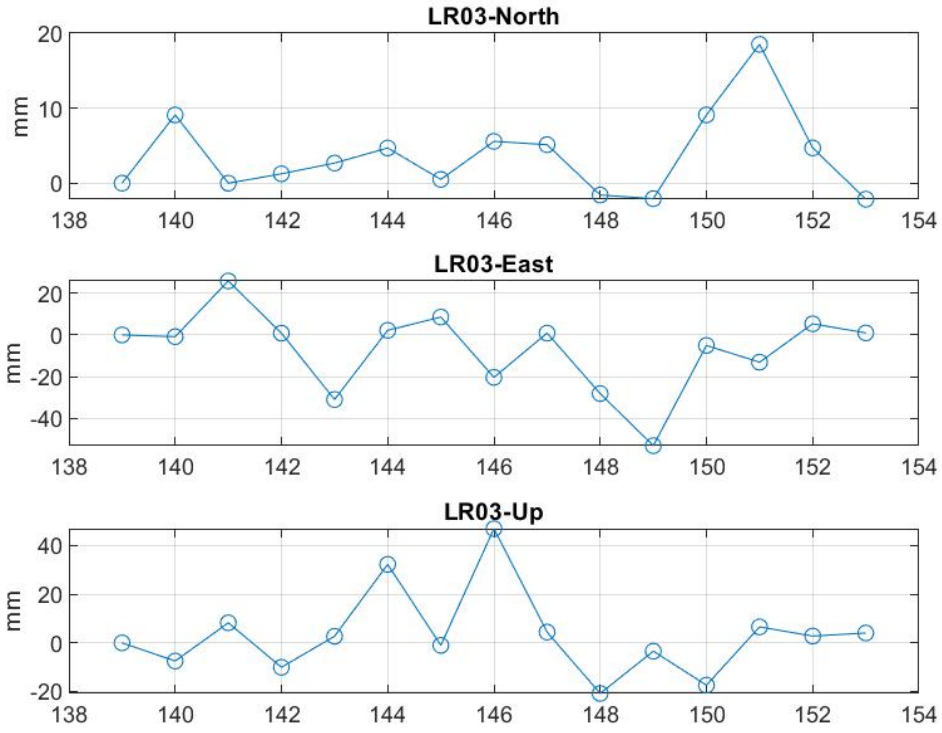


**Figure 36 LR03 station daily North, East and Up direction position**

In the table 17, we can see the coordinate day per day, processed in static mode, the red 146 doy represent the earthquake day, after that they change some centimeters as we can see in the figure 36 and table in mention. The coordinate is in ENU considering the first day as zero, the average coordinate before earthquake was 0.08 cm east and 0.26 north, after earthquake changed to 1.32 west and 0.45 north, in vertical component not much difference such as we can see in the table in mention.

**Table 17 LR03 station daily coordinate towards the east north and up direction (cm)**

| Doy | E | N | U |
|---|---|---|---|
| 139 | 0.00 | 0.00 | 0.00 |
| 140 | -0.08 | 0.91 | -0.75 |
| 141 | 2.59 | 0.00 | 0.83 |
| 142 | 0.08 | 0.12 | -1.00 |
| 143 | -3.10 | 0.27 | 0.27 |
| 144 | 0.22 | 0.47 | 3.23 |
| 145 | 0.86 | 0.05 | -0.10 |
| 146 | -2.03 | 0.56 | 4.70 |
| 147 | 0.09 | 0.51 | 0.44 |
| 148 | -2.81 | -0.16 | -2.08 |
| 149 | -5.31 | -0.21 | -0.34 |
| 150 | -0.51 | 0.91 | -1.74 |
| 151 | -1.31 | 1.85 | 0.66 |
| 152 | 0.53 | 0.47 | 0.28 |
| 153 | 0.10 | -0.21 | 0.41 |
| | **Average E** | **Average N** | **Average U** |
| **BE:** | 0.08 | 0.26 | 0.35 |
| **AE:** | -1.32 | 0.45 | -0.34 |
| **Δ:** | -1.40 | 0.19 | -0.69 |

Also, we can see the displacement occurred after earthquake, had 1.40 cm displacement

west component and 0.19 cm to the south, surrounding 1.5 cm in this last component, in vertical component 0.69 cm down.

### 5.3.10 LR06 station

LR06 station is 190 Km from epicenter earthquake, in the figure 37 we can see the movement along the time respect to earthquake, in North component we can see significative change along the time, and in the East component little change after earthquake, in the horizontal component the variability is surrounding 10 cm into 14 days processed.

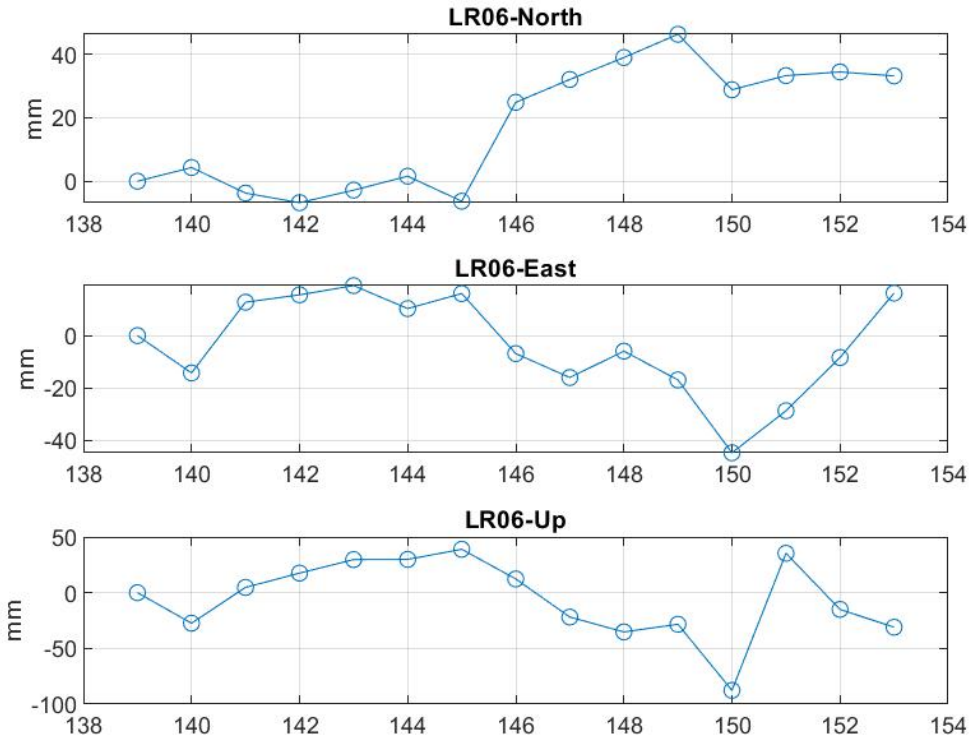


**Figure 37 LR06 station daily North, East and Up direction position**

In the table 18 we can see the coordinate day per day, processed in static mode, the red 146 doy represent the earthquake day, after that they change some centimeters as we can see in the figure 37 and table in mention. The coordinate is in ENU considering the first day as zero, the average coordinate before earthquake was 0.85 cm east and 0.20 south, after earthquake changed to 1.49 west and 3.53 north, in vertical component not much difference

such as we can see in the table in mention.

**Table 18 LR06 station daily coordinate towards the east north and up direction (cm)**

| Doy | E | N | U |
|---|---|---|---|
| 139 | 0.00 | 0.00 | 0.00 |
| 140 | -1.42 | 0.43 | -2.74 |
| 141 | 1.27 | -0.37 | 0.48 |
| 142 | 1.55 | -0.68 | 1.76 |
| 143 | 1.90 | -0.28 | 2.97 |
| 144 | 1.03 | 0.16 | 2.99 |
| 145 | 1.60 | -0.63 | 3.90 |
| 146 | -0.69 | 2.49 | 1.23 |
| 147 | -1.60 | 3.21 | -2.19 |
| 148 | -0.59 | 3.90 | -3.52 |
| 149 | -1.69 | 4.63 | -2.83 |
| 150 | -4.46 | 2.88 | -8.77 |
| 151 | -2.86 | 3.33 | 3.54 |
| 152 | -0.84 | 3.45 | -1.50 |
| 153 | 1.62 | 3.32 | -3.10 |
| | **Average E** | **Average N** | **Average U** |
| **BE:** | 0.85 | -0.20 | 1.34 |
| **AE:** | -1.49 | 3.53 | -2.62 |
| **Δ:** | -2.34 | 3.73 | -3.96 |

Also, we can see the displacement occurred after earthquake, had 2.34 cm displacement west component and 3.73 cm to the north, surrounding 3.7 cm in this last component, in vertical component 3.96 cm down.

### 5.3.11 LR07 station

LR07 station is 202 Km from epicenter earthquake, and this station is little same to SM02 and LR06 in radial distance from earthquake, in the figure 38 we can see the movement along the time respect to earthquake, in North component we can see little change along the time, and in the East component little change after earthquake, in the horizontal component the variability is rounding 4 cm into 14 days processed.

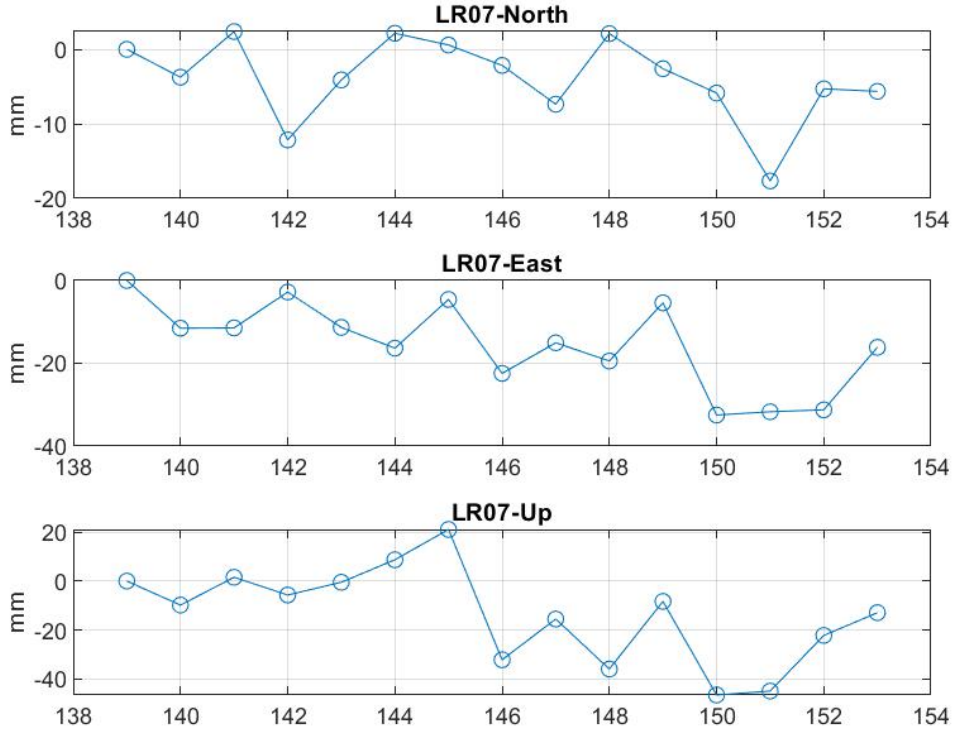


**Figure 38 LR07 station daily North, East and Up direction position**

In the table 19, we can see the coordinate day per day, processed in static mode, the red 146 doy represent the earthquake day, after that they change some centimeters as we can see in the figure 38 and table in mention. The coordinate is in ENU considering the first day as

zero, the average coordinate before earthquake was 0.83 cm west and 0.21 south, after earthquake changed to 2.16 west and 0.60 south, in vertical component we can see a little increasing the from up to down.

**Table 19 LR07 station daily coordinate towards the east north and up direction (cm)**

| Doy | E | N | U |
|---|---|---|---|
| 139 | 0.00 | 0.00 | 0.00 |
| 140 | -1.15 | -0.37 | -0.98 |
| 141 | -1.15 | 0.24 | 0.16 |
| 142 | -0.28 | -1.22 | -0.57 |
| 143 | -1.13 | -0.41 | -0.05 |
| 144 | -1.64 | 0.22 | 0.87 |
| 145 | -0.46 | 0.06 | 2.11 |
| 146 | -2.24 | -0.22 | -3.21 |
| 147 | -1.50 | -0.74 | -1.55 |
| 148 | -1.95 | 0.21 | -3.59 |
| 149 | -0.54 | -0.26 | -0.83 |
| 150 | -3.25 | -0.59 | -4.65 |
| 151 | -3.17 | -1.77 | -4.49 |
| 152 | -3.12 | -0.53 | -2.22 |
| 153 | -1.61 | -0.56 | -1.29 |
| | **Average E** | **Average N** | **Average U** |
| **BE:** | -0.83 | -0.21 | 0.22 |
| **AE:** | -2.16 | -0.60 | -2.66 |
| **Δ:** | -1.34 | -0.39 | -2.88 |

Also, we can see the displacement occurred after earthquake, had 2.86 cm displacement west component and 0.28 cm to the south, surrounding 2 cm in this last component, in vertical component 1.34 cm up.

### 5.3.12 SM01 station

SM01 station is 163 Km from epicenter earthquake, and this station is little same to LR02 in radial distance from earthquake, in the figure 39 we can see the movement along the time respect to earthquake, in North component we can see little change along the time south direction, and in the East component significative change after earthquake south direction, in the horizontal component the variability is rounding 7 cm into 14 days processed.

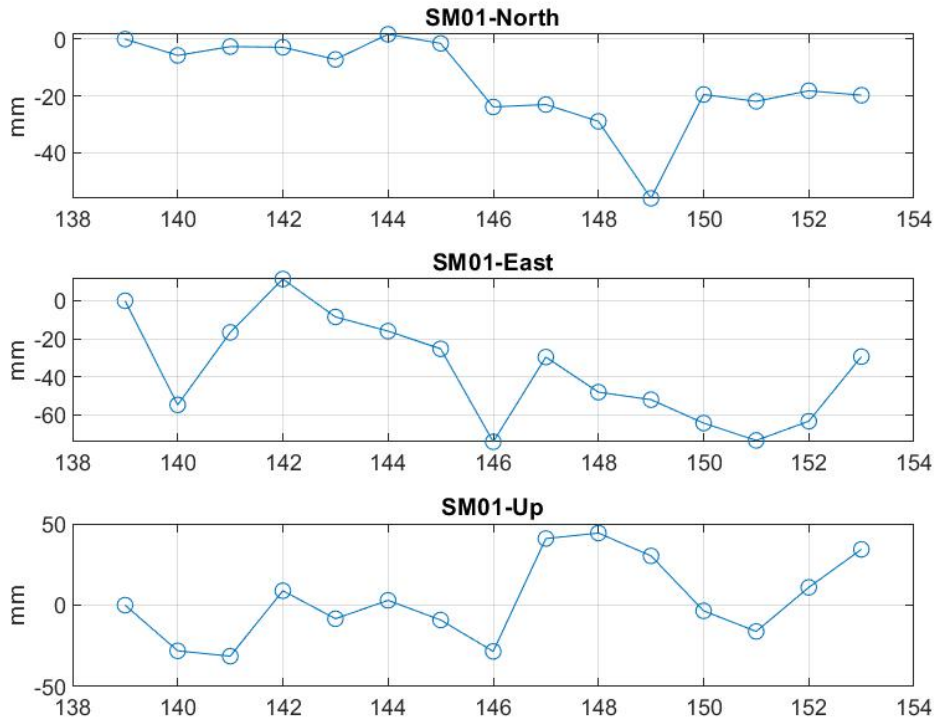


**Figure 39 SM01 station daily North, East and Up direction position**

In the table 20, we can see the coordinate day per day, processed in static mode, the red 146 doy represent the earthquake day, after that they change some centimeters as we can see in the figure 39 and table in mention. The coordinate is in ENU considering the first day as zero, the average coordinate before earthquake was 0.57 cm west and 0.26 south, after earthquake changed to 5.15 west and 2.76 south, in vertical component we can see a little increasing the from down to up.

**Table 20 SM01 station daily coordinate towards the east north and up direction (cm)**

| Doy | E | N | U |
|---|---|---|---|
| 139 | 0.00 | 0.00 | 0.00 |
| 140 | -5.48 | -0.57 | -2.80 |
| 141 | -1.67 | -0.26 | -3.13 |
| 142 | 1.14 | -0.29 | 0.89 |
| 143 | -0.85 | -0.71 | -0.83 |
| 144 | -1.60 | 0.17 | 0.30 |
| 145 | -2.53 | -0.15 | -0.91 |
| 146 | -7.43 | -2.38 | -2.84 |
| 147 | -2.96 | -2.30 | 4.09 |
| 148 | -4.81 | -2.89 | 4.43 |
| 149 | -5.21 | -5.60 | 3.03 |
| 150 | -6.44 | -1.95 | -0.35 |
| 151 | -7.35 | -2.19 | -1.62 |
| 152 | -6.34 | -1.82 | 1.09 |
| 153 | -2.94 | -1.97 | 3.43 |
| | **Average E** | **Average N** | **Average U** |
| **BE:** | -1.57 | -0.26 | -0.93 |
| **AE:** | -5.15 | -2.67 | 2.02 |
| **Δ:** | -3.58 | -2.41 | 2.94 |

Also, we can see the displacement occurred after earthquake, had 3.58 cm displacement west component and 2.41 cm to the south, rounding 2.5 cm in this last component, in vertical component 2.94 cm up.

### 5.3.13 SM02 station

SM02 station is 208 Km from epicenter earthquake, and this station is little same to LR06 and LR07 in radial distance from earthquake, in the figure 40 we can see the movement along the time respect to earthquake, in North component we can see little change along the time south direction, and in the East component significative change after earthquake south direction, but this points are some scattering along the time, in the horizontal component the variability is rounding 3 cm into 14 days processed.

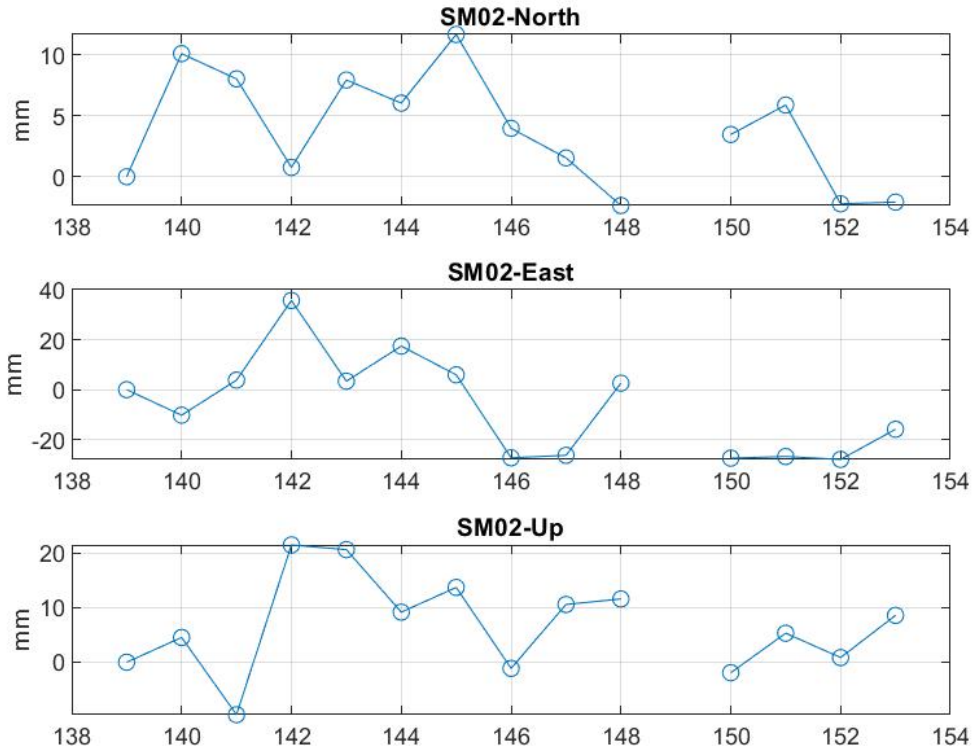


**Figure 40 SM02 station daily North, East and Up direction position**

In the table 21, we can see the coordinate day per day, processed in static mode, the red 146 doy represent the earthquake day, after that they change some centimeters as we can see in the figure 40 and table in mention. The coordinate is in ENU considering the first day as zero, the average coordinate before earthquake was 0.80 cm east and 0.64 north, after earthquake changed to 2.03 west and 0.07 north, in vertical component we can see constant

behavior.

**Table 21 SM02 station daily coordinate towards the east north and up direction (cm)**

| Doy | E | N | U |
|---|---|---|---|
| 139 | 0.00 | 0.00 | 0.00 |
| 140 | -1.02 | 1.01 | 0.45 |
| 141 | 0.38 | 0.80 | -0.96 |
| 142 | 3.57 | 0.08 | 2.15 |
| 143 | 0.34 | 0.79 | 2.06 |
| 144 | 1.74 | 0.60 | 0.92 |
| 145 | 0.59 | 1.17 | 1.37 |
| 146 | -2.73 | 0.40 | -0.11 |
| 147 | -2.63 | 0.15 | 1.06 |
| 148 | 0.26 | -0.24 | 1.16 |
| 149 | NaN | NaN | NaN |
| 150 | -2.74 | 0.35 | -0.19 |
| 151 | -2.68 | 0.59 | 0.53 |
| 152 | -2.79 | -0.22 | 0.08 |
| 153 | -1.58 | -0.21 | 0.86 |
| | **Average E** | **Average N** | **Average U** |
| **BE:** | 0.80 | 0.64 | 0.86 |
| **AE:** | -2.03 | 0.07 | 0.58 |
| **Δ:** | -2.83 | -0.57 | -0.27 |

Also, we can see the displacement occurred after earthquake, had 2.83 cm displacement west component and 0.57 cm to the south, rounding 1 cm in this last component, in vertical

component 0.27 cm down.

### 5.3.14 UC01 station

UC01 station is 316 Km from epicenter earthquake, and this station is little same to LB01 in radial distance from earthquake, in the figure 41 we can see the movement along the time respect to earthquake, in North component we can see significative change along the time, and in the East component like constant change after earthquake, in the horizontal component the variability is rounding 5 cm into 14 days processed.

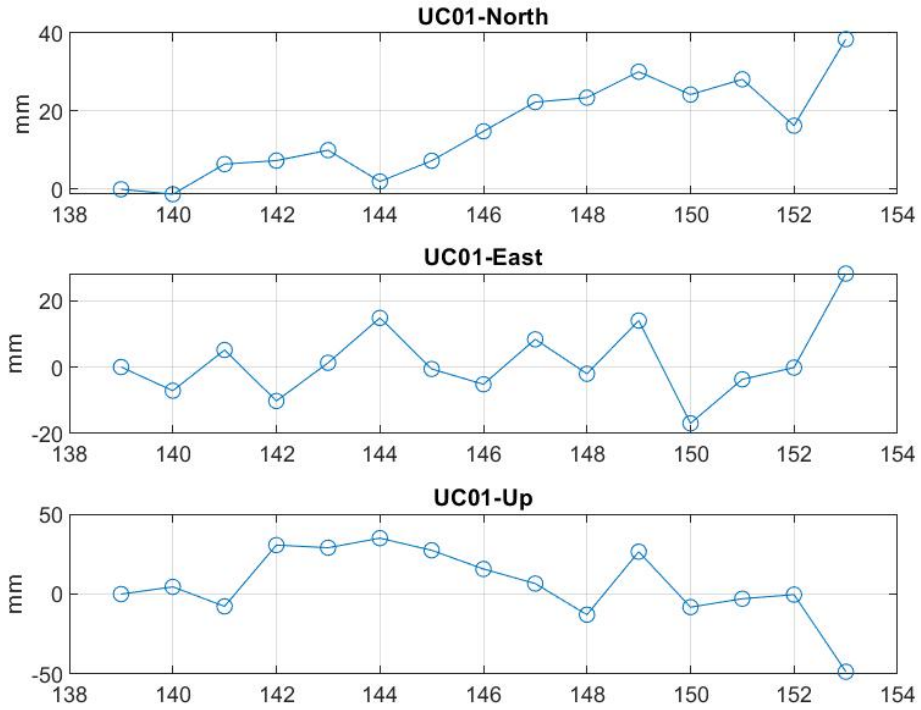


**Figure 41 UC01 station daily North, East and Up direction position**

In the table 22, we can see the coordinate day per day, processed in static mode, the red 146 doy represent the earthquake day, after that they change some centimeters as we can see in the figure 41 and table in mention. The coordinate is in ENU considering the first day as zero, the average coordinate before earthquake was 0.05 cm east and 0.45 north, after earthquake changed to 0.39 east and 2.61 north, in vertical component not much difference such as we can see in the table in mention.

**Table 22 UC01 station daily coordinate towards the east north and up direction (cm)**

| Doy | E | N | U |
|---|---|---|---|
| 139 | 0.00 | 0.00 | 0.00 |
| 140 | -0.71 | -0.13 | 0.45 |
| 141 | 0.51 | 0.64 | -0.77 |
| 142 | -1.02 | 0.73 | 3.06 |
| 143 | 0.13 | 1.00 | 2.90 |
| 144 | 1.48 | 0.20 | 3.50 |
| 145 | -0.06 | 0.73 | 2.74 |
| 146 | -0.52 | 1.48 | 1.57 |
| 147 | 0.83 | 2.23 | 0.66 |
| 148 | -0.20 | 2.35 | -1.29 |
| 149 | 1.40 | 3.01 | 2.65 |
| 150 | -1.69 | 2.42 | -0.81 |
| 151 | -0.37 | 2.82 | -0.29 |
| 152 | -0.02 | 1.63 | -0.03 |
| 153 | 2.81 | 3.84 | -4.85 |
| | **Average E** | **Average N** | **Average U** |
| **BE:** | 0.05 | 0.45 | 1.70 |
| **AE:** | 0.39 | 2.61 | -0.57 |
| **Δ:** | 0.35 | 2.16 | -2.27 |

Also, we can see the displacement occurred after earthquake, had 0.35 cm displacement east component and 2.16 cm to the north, rounding 2 cm in this last component, in vertical

component 2.27 cm down.

## 5.4 Average sum of carriers and pseudoranges

The advantages of combining both carrier and code measurements by this method will allow real-time calculations without the required convergence of the standard GPS techniques that may take several minutes to settle with similar precision.

In next table can show the average sum of carriers and pseudoranges of data processing

**Table 23 Average Sum (LC and PC SIGMA)**

| DAY | LC (mm) | PC (mm) |
|---|---|---|
| 139 | 8.882 | 1085.779 |
| 140 | 9.452 | 1084.510 |
| 141 | 8.858 | 1088.059 |
| 142 | 9.266 | 1086.857 |
| 143 | 10.024 | 1083.602 |
| 144 | 9.831 | 1095.415 |
| 145 | 9.707 | 1096.564 |
| 146 | 8.511 | 1100.031 |
| 147 | 8.717 | 1098.966 |
| 148 | 9.612 | 1088.982 |
| 149 | 10.228 | 1101.433 |
| 150 | 9.227 | 1087.958 |
| 151 | 9.427 | 1103.201 |
| 152 | 9.679 | 1070.083 |
| 153 | 10.844 | 1084.070 |

# Conclusion

The calculated results processed in PANDA software can us show the position behavior for 14 GNSS station for a long one week before and after earthquake 8 Mw magnitude; data processed precision is high accuracy into 10mm, each GNSS station have a different magnitude and direction in displacement surrounding earthquake, the most GNSS stations have a displacement to direction south west, these stations represent the 65% to a same direction, the other stations present little movements and another directions out to the zone.

The GNSS station with more displacement is the AM01 with 5.27 cm to the west and 1.15 cm to the south, the AM05 with 4.2 cm to the west and 0.95 cm to the south, the CJ02 with 3.64 cm to the west and 0.68 cm to the south, the other stations had a little movement respect the average position before earthquake. In another hand the GNSS stations such have a little displacement was HC03 with 0.73 cm west and 0.17 cm south and the LR01 with 0.5 cm to the east and 0.84 to the north.

In this research the conclusion is the high accuracy data processing can show us good results for show the behavior and displacements in GNSS points, very important to know the difference of displacements and using this information's por geodesy and topography works, for high precision engineering jobs.

# References

[1] Alim Sikder M. A., Wu F. and Zhao Y., "Displacement Monitoring of CORS Reference Stations Using GNSS Precise Point Positioning in Bangladesh," 2018 14th IEEE International Conference on Signal Processing (ICSP), Beijing, China, 2018, pp. 1060-1064, doi: 10.1109/ICSP.2018.8652448.

[2] Savšek-Safić, S., Ambrožič, T., Stopar, B., & Turk, G. (2006). Determination of point displacements in the geodetic network. Journal of surveying engineering, 132(2), 58-63. doi:10.1061/(asce)0733-9453(2006)132:2(58).

[3] Decker, B. L. (1986). World geodetic system 1984. Defense Mapping Agency Aerospace Center St Louis Afs Mo.

[4] Drewes H. (2009) Reference Systems, Reference Frames, and the Geodetic Datum. In: Sideris M.G. (eds) Observing our Changing Earth. International Association of Geodesy Symposia, vol 133. Springer, Berlin, Heidelberg. https://doi.org/10.1007/978-3-540-85426-5_1.

[5] Zheng, G., Wang, H., Wright, T.J., Lou, Y., Zhang, R., Zhang, W., Shi, C., Huang, J. and Wei, N., 2017. Crustal deformation in the India‐Eurasia collision zone from 25 years of GPS measurements. Journal of Geophysical Research: Solid Earth, 122(11), pp.9290-9312.

[6] Teferle, F.N., Orliac, E.J. & Bingley, R.M. An assessment of Bernese GPS software precise point positioning using IGS final products for global site velocities. GPS Solutions 11, 205–213 (2007). https://doi.org/10.1007/s10291-006-0051-7.

[7] Gao, Y., Zhang, Y., & Chen, K. (2006, September). Development of a real-time single-frequency precise point positioning system and test results. In Proceedings of Ion GNSS (pp. 26-29).

[8] Abdel-salam M. A., “Precise Point Positioning Using Un-Differenced Code and Carrier Phase Observations,” Deparment Geomatics Eng., vol. Docter of, no. 20229, p. 228, 2005.

[9] Hobbs D. and Bohn P., “Precise Orbit Determination for Low Earth Orbit Satellites,” Ann. Marie Curie Fellowsh. Assoc., vol. 4, no. 1, pp. 1–7, 2006.

[10] Ge M., Gendt G., Dick G., Zhang F. P., and Rothacher M., “A new data processing strategy for huge GNSS global networks,” J. Geod., vol. 80, no. 4, pp. 199–203, 2006.

[11] Afifi A. and El-rabbany A., “Un-differenced precise point positioning model using triple GNSS constellations,” Cogent Geosci., 2016.

[12] Engineering G., "UCGE Reports Precise Point Positioning Using Dual-Frequency GPS and GLONASS Measurements," Processing, no. 20291, 2009.

[13] Kouba J. and Héroux P., "GPS Precise Point Positioning Using IGS Orbit Products," Phys. Chem. Earth, Part A Solid Earth Geod., 2000.

[14] Larson KM (2009) GPS seismology. J Geod 83:227–233.

[15] Larson KM, Bodin P, Gomberg J (2003) Using 1-Hz GPS data to measure deformations caused by the Denali fault earthquake. Science 300:1421–1424.

[16] Kouba J (2003) Measuring seismic waves induced by large earthquakes with GPS. Stud Geophys Geod 47:741–755.

[17] Berné, J. L., Anquela Julián, A. B., and Natalia, V. G. (2014). GNSS. GPS: fundmentos y aplicaciones en Geomática. Univeridad Politécnica de Valencia, primera edition.

[18] Hofmann-Wellenhof, B., Lichtenegger, H., Collins, J., Hofmann-Wellenhof, B., Lichtenegger, H., and Collins, J. (2011). Mathematical models for positioning. In Global Positioning System, pages 181–202. Springer Vienna, Vienna.

[19] Valero, J. L. B., Villén, N. G., and Romá, R. C. (2019). GLONASS, BEIDOU Fundamentos y métodos de posicionamiento.

[20] Fernández Plazaola, U. (2003). Técnicas de resolución de la ambigüedad de las medidas de fase en sistemas de navegación por satélite. PhD thesis, Universidad de Málaga.

[21] Zumberge J. F., M. Heftin B., D. Jefferson C., and M. M. Watkins, "Precise point positioning for the efficient and robust analysis of GPS data from large networks -," J. Geophys. Res., vol. 102, no. 1, pp. 5005–5017, 1997.

[22] Gao Y. and Chen K., "Performance Analysis of Precise Point Positioning Using Rea-Time Orbit and Clock Products," J. Glob. Position. Syst., vol. 3, no. 1&2, pp. 95–100, 2010.

[23] Abou-Galala M., Rabah M., Kaloop M., and Z. Zidan M., "Assessment of the accuracy and convergence period of Precise Point Positioning," Alexandria Eng. J., vol. 57, no. 3, pp. 1721–1726, 2018.

[24] Satirapod C., "Comparing stochastic models used in GPS precise point positioning technique," Surv. Rev., vol. 308, no. April 2008, pp. 188–194, 2016.

[25] Leick A., GPS satellite Surveying Fourth Edition. 2004.

[26] Xu Y., "GNSS Precise Point Positioning with Application of the Equivalence Principle," no. September 2016.

[27] Becerra G., “Analysis of Stochastic Properties,” Geod. Sci. Surv. Tho Ohio State Univ., no. 490, p. Report No. 490, 2008.

[28] Alinia H. S., “New GPS Time Series Analysis and a Simplified Model to Compute an Accurate Seasonal Amplitude of Tropospheric Delay,” Electron. Thesis Diss. Repos., no. 4956, p. 239, 2017.

[29] Schmid R., “How to Use IGS Antenna Phase Center Corrections,” pp. 2005–2008, 2010.

[30] Zhu S. Y., Massmann F., Yu Y., and Reigber C., “Satellite antenna phase center offsets and scale errors in GPS solutions,” pp. 668–672, 2003.

[31] El-hattab A. I., “Influence of GPS antenna phase center variation on precise positioning,” NRIAG J. Astron. Geophys., no. December 2013, 2014.

[32] Agnew D. C., “Earth Tides. Treatise on Geophysics and Geodesy,” 2007.

[33] Yin H., Li J., Ma P., Zhang S., and Xu D., Geod. Geodyn., vol. 1, no. 1, pp. 64–69, 2010.

[34] Kouba J. and Héroux P., “Precise Point Positioning Using IGS Orbit and Clock Products,” GPS Solut., vol. 5, no. 2, pp. 12–28, 2001.

[35] Gao Y., Zhang Y., and Chen K., “Development of a Real-Time Single-Frequency Precise Point Positioning System and Test Results,” no. September, pp. 26–29, 2006.

[36] Bakker P. F., “On User Algorithms for GNSS Precise Point Positioning,” Delft Univ. Technol., p. 316, 2016.

[37] Soop E. M. and Soop E. M., Orbit Determination. 2013.

# Acknowledgments

My deepest gratitude goes first and foremost to Professor Shi Chuang, my supervisor, for his constant encouragement and guidance. He has walked me through all the stages of the writing of this thesis. Without his consistent and illuminating instruction, this thesis could not have reached its present form.

Second, I would like to express my heartfelt gratitude to Dr. Fan Lei, who led me into PANDA software for GNSS data processing. I am also greatly indebted to the professors and teachers at the International School, they teach me about Knowledges in my major and China culture.

Last my thanks would go to my beloved family for their loving considerations and great confidence in me all through these years. To my colleges in my country, they gave me their technical recommendation in this major. I also owe my sincere gratitude to my friends and my fellow classmates who gave me their help and time in listening to me and helping me work out my problems during the difficult course of the thesis.